CANADIAN THESES

THÈSES CANADIENNES

NOTICE

The quality of this microfiche is heavily dependent upon the quality of the original thesis submitted for microfilming. Every effort has been made to ensure the highest quality of reproduction possible.

If pages are missing, contact the university which granted the degree.

Some pages may have indistinct print especially if the original pages were typed with a poor typewriter ribbon or if the university sent us an inferior photocopy.

Previously copyrighted materials (journal articles, published tests, etc.) are not filmed.

Reproduction in full or in part of this film is governed by the Canadian Copyright Act, R.S.C. 1970, c. C-30. Please read the authorization forms which accompany this thesis.

AVIS

La qualité de cette microfiche dépend grandement de la qualité de la thèse soumise au microfilmage. Nous avons tout fait pour assurer une qualité supérieure de reproduction.

S'il manque des pages, veuillez communiquer avec l'université qui a conféré le grade.

La qualité d'impression de certaines pages peut laisser à désirer, surtout si les pages originales ont été dactylographiées à l'aide d'un ruban usé ou si l'université nous a fait parvenir une photocopie de qualité inférieure.

Les documents qui font déjà l'objet d'un droit d'auteur (articles de revue, examens publiés, etc.) ne sont pas microfilmés.

La reproduction, même partielle, de ce microfilm est soumise à la Loi canadienne sur le droit d'auteur, SRC 1970, c. C-30. Veuillez prendre connaissance des formules d'autorisation qui accompagnent cette thèse.

THIS DISSERTATION HAS BEEN MICROFILMED EXACTLY AS RECEIVED

LA THÈSE A ÉTÉ MICROFILMÉE TELLE QUE NOUS L'AVONS REÇUE

Stability of the Electron Bubble in Rare Gas Solids

by

Louis Emery

Thesis submitted to the School of Graduate Studies
of the University of Ottawa in partial fulfilment
of the requirements for the degree
of Master of Science in Physics

Physics Department
Science and Engineering Faculty
University of Ottawa
Ottawa, Canada
1983

Remerciements

J'aimerais remercier Dr K.S.Song, directeur de thèse, pour son enseignement, son encouragement et sa patience lors de la réalisation du projet. I would also like to thank Dr C.H.Leung for his part in tutoring me in the various calculational methods used in the work. I feel privileged to have been associated with these persons, as I found that they produced an excellent working environment, which is indispensable to me.

Thanks goes to L.K.Moleko and Dr H.G.Glyde for interesting conversations relating to the difficult problem of zero-point energy motion.

Certains calculs numériques faits par les étudiants d'été D.Masson et G.Kelly, qui apparaissent dans cette thèse sont également appréciés.

Enfin, je tiens a remercier mes amis, ma mère et les autres membres de ma famille pour leurs encouragements tout au long de mes études.

Ce travail fut réalisé grace au support du Conseil National de Recherches du Canada.

Table of Contents

Chapter I

Description of the Problem

In this thesis we report a calculation which determines the relative stability of two types of excited electron states in rare gas solids (RGS) : the electron bubble and the lowest energy conduction state. To the author's knowledge no theoretical work has ever been published concerning this, although there is published experimental evidence[1-3] which is very closely related to this problem. The relative stability of one state is deduced from the measurement of the negative charge carrier mobility in the rare gas solid. These values indicate that the the conduction state is the stable one for Neon, Argon and Krypton solids (these are the rare gas solids which are to be treated in this thesis). The same thing holds for the rare gases in liquid form with the exception of liquid Neon, where the electron bubble is stable. These experimental findings will be used to confirm our results.

We shall use a new pseudopotential method of treating these excited electron states. This one-electron Hartree-Fock method has been used for the Rydberg series of rare gas and alkali atoms and for the self-trapped exciton bubble in solid Ne with success.[4,5]

Of the two states, the electron bubble is of the most interest because an atomistic approach is used rather than a continuum approximation of the solid as in the electron bubble theory in liquid rare gases. Conduction bands in RGS have been calculated by many workers with different methods.[22-34,41] Our pseudopotential, which was initialy developped to treat electronic defects in

insulators, can be easily extended to calculate conduction bands for insulators.

Our electron bubble model is as follows. Around an electron localized within a solid, the neighbouring atoms will undergo outward displacements which form the cavity. The electron is presumably lodged on a vacancy site. It is also possible that the electron places itself on an interstitial site, but this is considered less probable than the former mostly because of the large concentration of vacancies in RGS at thermal equilibrium at high temperature. The reason for the repulsion of the surrounding atoms is this. The interaction between the defect electron and the atoms is two-fold. In our Hamiltonian we have a repulsive term and an attractive term. The repulsive term arises from the orthogonality requirement of the defect electron wavefunction with respect to all other core electron wavefunctions. The attractive part includes the polarization energy (defect has net charge -e), the short range coulomb and exchange energy and, to a lesser extent, deformation energy. Considering these factors we expect that the repulsion term overpowers the attractive term in light inert gas cases. In the heavier rare gases, the atomic polarizability is much larger making the effect of the excess electron on the atoms less repulsive. In reference 6 are listed the experimental electronic affinities of the rare gas atoms. The values for Ne, Ar and Kr are, respectively, -1.4, -0.4 and 0.3 eV. Ignoring for the moment that electron bubbles could be unstable this means that the size of the defect's cavity should increase as the atomic number of the rare gas decreases. This tendency should appear in our results.

To determine the relative stability of the two possible states, we simply compare their respective thermodynamic free energies, and the lowest one will be that of the stable state. The energy of the bubble is taken to be the sum of the electronic energy of the defect, the polarization energy and the lattice deformation energy. The energy of the extended state will include the polarization or correlation energy as calculated by a method based on previous works in RGS band calculations.

It seems appropriate to briefly compare this thesis's treatment of the stability problem as applied to RGS with the treatment from earlier works (refs 7,8) of the stability problem as applied to rare gas liquids (RGL). These works report that the excess electron state in RGL of atomic number greater than that of Ne should be quasifree (i.e. a conduction state) while the Ne liquid case was found to be unlikely, or at best, uncertain. We expect qualitatively the same tendency for the solid case. The fundamental difference is their use of the continuum approximation of the liquid. For the liquid this seems to be the practical approach since an atomistic one would be complicated by the energetic motion of the atoms. In the continuum approximation the stability criteria are given in terms of liquid density, surface tension, atomic polarizability and atomic scattering length (with polarization effects excluded). In their model of the electron model the number density of atoms around the electron makes an abrupt change at some radius, the density being zero inside the cavity and equal to the equilibrium density outside the cavity. The potential energy within the sphere is taken to be a constant with respect to that of the liquid. This energy is estimated from

experimental scattering length. For the surface tension, experimental bulk values is used and any structure or 'fuzziness' of the surface of the cavity is ignored. To determine the polarization effects the liquid is approximated by a continuous medium of a given dielectric constant.

The main motivation of our calculation was the application of the new hybrid pseudopotential with 1-s gaussian bases to a type of electronic defect even though it turns out unstable.

Chapter II

Bubble Calculation

There are three distinct parts to the electron bubble problem. As mentioned in the first chapter, the electronic sctructure is combined with the polarization effects and the atomic displacements around the defect. The following sections contain the general formulation of the theories involved and also the details on the application to our specific problem.

Section I Electronic Structure

A rigorous treatment of the excess electron in an insulator would require that all the electron states of the crystal be determined self-consistently. However, it is observed that the occupied core electron states are much more tightly bound than the state associated with the defect. Thus we can assume that the excited states are determined by the existing core states while the latter remain unchanged by the presence of the extra electron. Whatever changes that inevitably occur fall under the heading of polarization effects.

The above assumption results in a vast simplification. Two models exploiting this are of particular interest: the extended-ion model and the ion-size model, the latter being an approximation of the former. Both models involve solving the one-elctron Hartree-Fock equation of the defect system. The HF Hamiltonian is

$$H = -\frac{1}{2}\nabla^2 + V_{PI}(\vec{r}) + V_{sc}(\vec{r}) + V_{ex}(\vec{r}) \qquad (1)$$

where $$V_{ez}(\vec{r}) = -\sum_{\gamma} \frac{\tilde{Z}_\gamma}{|\vec{r} - \vec{R}_\gamma|} \quad , \tag{2}$$

$$v_{sc} = \sum_{\gamma} V_{sc,\gamma} = -\sum_{\gamma} \frac{Z_\gamma - \tilde{Z}_\gamma}{|\vec{r} - \vec{R}_\gamma|} + 2\int \sum_{\lambda}^{n_\lambda} \frac{|\chi_{\gamma,\lambda}(\vec{r}_2)|^2}{|\vec{r} - \vec{r}_2|} d\vec{r}_2 \quad , \tag{3}$$

$$v_{ex} = \sum_{\gamma} V_{ex,\gamma} = -\sum_{\gamma,\lambda} \int \frac{\chi_{\gamma,\lambda}(\vec{r}_1)\, \chi^*_{\gamma,\lambda}(\vec{r}_2)\, \rho_{1,2}}{r_{12}} d\vec{r}_2 \tag{4}$$

and $\vec{r}$ is the defect electron position vector, $\vec{R}_\gamma$ is the position of the γ th lattice site, $\chi_{\gamma,\lambda}$ is the λ th (doubly) occupied atomic orbital on the γ th atom, Z_γ is the nuclear charge, $\tilde{Z}_\gamma$ is the total charge of the ion or atom. The summation in γ includes all the atoms present in the problem. An important point can be made here about the Hamiltonian. In Wood and Joy,[9] the Coulomb and exchange integrals are originally defined from the Fock-Dirac density matrix formalism:

$$\rho(1,2) = \sum_{\gamma=0}^{N} \sum_{\lambda}^{n_\lambda} \chi_{\gamma,\lambda}(1)\, \chi^*_{\gamma,\lambda}(2) \tag{5}$$

The difference with our Hamiltonian is the term $\chi_{0,1}(1)\,\chi_{0,1}(2)$ which is the density of the defect electron itself. Wood and Joy determined that this contribution is exactly zero, and thus this term can be ignored in the Hamiltonian. Atomic units ($e = h = m = 1$) are used throughout. We assume the χ's to be free atomic HF orbitals taken from the Clementi and Roetti wavefunction tables[10] which means that we neglect any change that actually occur to the core wavefunctions as the atoms are brought together to form a solid and as the atoms are pushed around in the process of creating the cavity. Also, any account of the polarization is phenomenological; the wavefunctions will stay unperturbed in the presence

of the excess electron. Since the overlap between core orbitals is small provided that it doesn't vanish from symmetry, we will assume that it is zero.

The defect electron will be a linear combination of an orthogonalized floating gaussian bases Ψ_i :

$$|\psi_i\rangle = |\phi_i\rangle - \sum_{r,\lambda} |\chi_{r,\lambda}\rangle\langle\chi_{r,\lambda}|\phi_i\rangle \qquad (6)$$

where ϕ_i is a ls-type gaussian function. We qualify the Ψ_i's as a floating bases because in placing them judiciously on or around the defect center, we can treat as many different symmetries of excited states we want.

The energies and the defect wavefunctions may be obtained by solving the secular equation

$$|H_{ij} - E S_{ij}| = 0 \qquad (7)$$

where

$$H_{ij} = \langle\Psi_i|H|\Psi_j\rangle \qquad (8)$$

and

$$S_{ij} = \langle\Psi_i|\Psi_j\rangle \qquad (9)$$

In other words, the H and S matrices must be diagonalized simultaneously because the bases are not mutually orthogonal. Substituting (6) in (8) and (9) gives

$$\begin{aligned} H_{ij} = {} & \langle\phi_i|H|\phi_j\rangle - \sum_{r,\lambda}\langle\phi_i|\chi_{r,\lambda}\rangle\langle\chi_{r,\lambda}|H|\phi_j\rangle \\ & - \sum_{r,\lambda}\langle\chi_{r,\lambda}|\phi_j\rangle\langle\phi_i|H|\chi_{r,\lambda}\rangle \\ & + \sum_{r}\sum_{r,\lambda}\langle\chi_{r',\lambda'}|\phi_j\rangle\langle\phi_i|\chi_{r,\lambda}\rangle\langle\chi_{r,\lambda}|H|\chi_{r',\lambda'}\rangle \end{aligned} \qquad (10)$$

$$S_{ij} = \langle \phi_i | \phi_j \rangle - 2\sum_{\gamma\lambda} \langle \phi_i | \chi_{\gamma,\lambda} \rangle \langle \chi_{\gamma,\lambda} | \phi_j \rangle$$
$$+ \sum_{\gamma\lambda} \sum_{\gamma'\lambda'} \langle \phi_i | \chi_{\gamma\lambda} \rangle \langle \chi_{\gamma'\lambda'} | \phi_j \rangle \langle \chi_{\gamma\lambda} | \chi_{\gamma'\lambda'} \rangle \qquad (11)$$

In rare gas solids, the atoms are neutral ($\bar{Z} = 0$), then $V_{ex} = 0$ and

$$\langle \phi_i | H | \phi_j \rangle = \langle \phi_i | -\tfrac{1}{2}\nabla^2 | \phi_j \rangle + \langle \phi_i | (V_{sc} + V_{Ex}) | \phi_j \rangle \qquad (12)$$

Rewrite the operator H in $\langle \chi_{\gamma\lambda} | H | \chi_{\gamma'\lambda'} \rangle$ and in $\langle \chi_{\gamma\lambda} | H | \phi_j \rangle$ as a sum of two parts: the effective Hamiltonian for the λth orbital on the γth atom and the part which remains.

$$\langle \chi_{\gamma\lambda} | H | \chi_{\gamma'\lambda'} \rangle = \langle \chi_{\gamma\lambda} | H_{\gamma\lambda} | \chi_{\gamma'\lambda'} \rangle + \langle \chi_{\gamma,\lambda} | H - H_{\gamma\lambda} | \chi_{\gamma'\lambda'} \rangle \qquad (13)$$

but $$H_{\gamma,\lambda} | \chi_{\gamma,\lambda} \rangle = \varepsilon_\lambda^\circ | \chi_{\gamma,\lambda} \rangle \qquad (14)$$

where $\varepsilon_\lambda^\circ$ is the HF orbital energy taken from Clementi wavefunction tables. Since the overlap between core electrons is small, we have : (see Appendix of ref. 9)

$$\langle \chi_{\gamma\lambda} | H | \chi_{\gamma\lambda'} \rangle = \varepsilon_\lambda^\circ \delta_{\gamma\gamma'} \delta_{\lambda\lambda'} \qquad (15)$$

and $$\langle \chi_{\gamma\lambda} | H - H_{\gamma\lambda} | \chi_{\gamma'\lambda'} \rangle = 0 \qquad (16)$$

where we take $$\langle \chi_{\gamma\lambda} | \chi_{\gamma'\lambda'} \rangle = \delta_{\lambda\lambda'} \delta_{\gamma\gamma'} \qquad (17)$$

Using the same arguments for $\langle \chi_{\gamma,\lambda} | H | \phi_j \rangle$ we get

$$\langle \chi_{\gamma,\lambda} | H | \phi_j \rangle = \varepsilon_\lambda^\circ \langle \chi_{\gamma,\lambda} | \phi_j \rangle \qquad (18)$$

The resulting matrix elements look like this:

$$H_{ij} = (K.E.)_{ij} + \left(\sum_\gamma V_{ex,\gamma} + \sum_\gamma V_{sc,\gamma}\right)_{ij}$$
$$- \sum_{\gamma,\lambda} \varepsilon_\lambda^\circ \langle \phi_i | \chi_{\gamma\lambda} \times \chi_{\gamma,\lambda} | \phi_j \rangle \qquad (19)$$

$$S_{ij} = \langle \phi_i | \phi_j \rangle + \sum_{\gamma,\lambda} \langle \phi_i | \chi_{\gamma,\lambda} \rangle \langle \chi_{\gamma,\lambda} | \phi_j \rangle \qquad (20)$$

In the right hand side of equations (19) and (20) all terms

excluding the kinetic energy and the gaussian overlap are the ion-size correction terms contributed by all the atoms present. In later expressions $V_{s\ell}(\vec{r})$ and $V_{s\ell}(\vec{r})$ will represent the potentials produced by a single atom. In the case where ions are present in the system their effects will be included as a correction term added to $\varepsilon_\lambda^\circ$ (i.e. $\varepsilon_\lambda = \varepsilon_\lambda^\circ + \Delta\varepsilon_\lambda$)."

In the above the easy integrals to evaluate are $(K.E.)_{ij}$ and $\langle \phi_i | \phi_j \rangle$ since the ϕ's are 1s-type gaussians. The other integrals can become quite cumbersome especially for defect systems in which lattice relaxations are important and both lattice and electronic energy have to be calculated self-consistently. To simplify the electronic calculation, some pseudopotential theories have been proposed. Bartram et al's[11] (BSG) ion-size theory assumes that the pseudowavefunction varies slowly over the region of an atomic core. The atomic pseudopotentials are defined in terms of two ion-size parameters that are properties of the ions (or atoms) alone. BSG have calculated the lowest order ion-size parameters and later Zwicker[12] extended their theory to include the next higher order parameters. The pseudopotential used by BSG doesn't permit an easy definition of parameters of higher order. The straight orthogonalization approach as used by Zwicker, however, makes it simpler to obtain higher order parameters.

I-a) Slow Varying Approximation:

Suppose that we must evaluate the overlap integral:

$$\sum_{\lambda}^{n_\lambda} |\langle \phi(|\vec{r}-\vec{R}_o|) | \chi_{\gamma\lambda}(\vec{r}) \rangle|^2 \qquad (2.1)$$

To clearly show the approximation we take the simple case where i=j and $R_i = R_j = R_o$. We expand ϕ about the site R_o in a multipolar

series:

$$\phi(|\vec{r}-\vec{R}_0|) = \sum_{\ell} \frac{(2\ell+1)}{2} F_\ell(r, R_0) P_\ell(\cos\Omega_0)$$
$$= 2\pi \sum_{\ell} F_\ell(r, R_0) \sum_{m} \left[Y^*_{\ell m}(\hat{r}) Y_{\ell m}(\hat{R}_0) \right] \qquad (22)$$

where $$F_\ell(r, R_0) = \int_{-1}^{1} \phi(|\vec{r}-\vec{R}_0|) P_\ell(\cos\Omega) d(\cos\Omega_0) \qquad (23)$$

and Ω_0 is the angle between $\vec{r}$ and $\vec{R}_0$. We write out the overlap integral placing the core site at the origin and redefining $\vec{R}_0$ as the vector joining the pseudofunction to the core site: (24)

$$\langle \phi(|\vec{r}-\vec{R}_0|) | \chi_\lambda(r) \rangle = 2\pi \langle F_0 Y^*_{00}(\hat{r}) Y_{00}(\hat{R}_0) + F_1 Y^*_{10} Y_{10} + \cdots \; | \chi_\lambda(r) \rangle$$

The angular part of the above integral can be readily evaluated. For a core state of angular momentum l' only the F_ℓ's of l=l' will remain non-zero. The radial part is treated by applying the slowly varying approximation on F_ℓ. This is equivalent to saying that F_ℓ is smooth also. By expanding $F_\ell(r,R_0)$ in a Taylor's series about the core site(r=0). we obtain: (25)

$$\int F_\ell(r, R_0) R_{\gamma\lambda}(r) r^2 dr = \sum_n F^{(n)}_\ell(0, R_0) \frac{1}{n!} \int R_{\gamma\lambda}(r) r^{n+2} dr$$

where $R_{\gamma\lambda}(r)$ is the radial part of the core orbital $\chi_{\gamma\lambda}$ and $F^{(n)}_\ell$ is the nth derivative of F_ℓ. The first factor depends only on the pseudofunction while the second one depends on the core orbitals and constitutes the ion-size parameters. It is easy to show that for gaussian-type ϕ's the nonzero terms of the above expression are $F^{(\ell)}_\ell$, $F^{(\ell+2)}_\ell$ and so on. For radial functions which has a discontinuity in its derivative at the point R_0, for example, a Slater function at r=0, this isn't so.

After a little manipulation we obtain the following expression for the two lowest order ion-size terms of the overlap

at the atomic site :

$$\sum_\lambda |\langle \phi(|r-R_o|)|\chi_\lambda(r)\rangle|^2 = \frac{1}{4}|F_o(o,R_o)|^2 B + \frac{1}{4}F_o(o,R_o)F_o^{(2)}(o,R_o)\,K' + \frac{9}{4}|F_1^{(1)}(o,R_o)|^2 K + \ldots \quad (26)$$

where

$$B = \sum_{\substack{\lambda \\ s\text{-core}}} \left(\int \chi_\lambda \, d\tau\right)^2 \quad (27)$$

$$K' = \sum_{\substack{\lambda \\ s\text{-core}}} \left(\int \chi_\lambda \, d\tau\right)\left(\int \chi_\lambda \, r^2 d\tau\right) \quad (28)$$

$$K = \sum_{\substack{\lambda \\ p\text{-core}}} \left(\int r\cos\theta \, \chi_\lambda \, d\tau\right)^2 \quad (29)$$

For the off-diagonal element we get

$$\sum_\lambda \langle \phi_i(|\vec{r}-\vec{R}_i|)|\chi_\lambda(r)\rangle\langle \chi_\lambda(r)|\phi_j(|\vec{r}-R_j|)\rangle \quad (30)$$
$$= \frac{1}{4}F_{oi}(o,R_i)F_{oj}(o,R_j)\,B + \frac{1}{8}\left[F_{oi}(o,R_i)F_{oj}^{(2)}(o,R_j) + F_{oi}^{(2)}(o,R_i)F_{oj}(o,R_j)\right]K' + \frac{9}{4}F_{1i}^{(1)}(o,R_i)F_{1j}(o,R_j)\,\hat{R}_i\cdot\hat{R}_j\,K$$

where $F_{\ell i}^{(n)}$ are the expansion terms of ϕ_i and $F_{\ell j}^{(n)}$ are the ones for ϕ_j. The factor $\hat{R}_i\cdot\hat{R}_j$ does not appear in the diagonal element (equn 26) because $\hat{R}_o\cdot\hat{R}_o = 1$. The derivation of the above terms is given in Appendix C. The ion-size parameters B, K, K' do not change since we are still dealing with the same atomic site; it is only the pseudowavefunction that changes. If the lattice were composed of more than one tvpe of atom we would have to define additional parameters corresponding to the B, K and K'.

A similar treatment can be applied to the V_{sc} and the V_{ex} term and to the same order as above, we get:

$$(V_{sc} + V_{Ex})_{ij} = \frac{1}{4} F_{oi}(o,R_i) F_{oj}(o,R_j) A_o$$
$$+ \frac{1}{8}\left[F_{oi}(o,R_i) F_{oj}^{(2)}(o,R_j) + F_{oj}(o,R_j) F_{oi}^{(2)}(o,R_i)\right] J_o'$$
$$+ \frac{9}{4} F_{it}^{(1)}(o,R_i) F_{ij}^{(1)}(o,R_j) \hat{R}_i \cdot \hat{R}_j \; J_o + \ldots \qquad (31)$$

where

$$A_o = \int (V_{sc} + V_{Ex})\, d\tau \qquad (32)$$

$$J_o' = \int (V_{sc} + V_{Ex})\, r^2 d\tau \qquad (33)$$

$$J_o = \int r\cos\theta (V_{sc} + V_{Ex}) r\cos\theta\, d\tau \qquad (34)$$

It should be noted that because the exchange is a non-local operator J' is not proportional to J as would be the case if only V_{sc} was present inside the integral. Following Zwicker's work, the contribution of the short range potential and the overlap terms are combined to define the ion-size parameters:

$$A = A_o - \sum_{s\,core} \varepsilon_\lambda^o \, B_\lambda \qquad (35)$$

$$J' = J_o' - \sum_{s\,core} \varepsilon_\lambda^o \, K'_\lambda \qquad (36)$$

$$J = J_o - \sum_{p\,core} \varepsilon_\lambda^o \, K_\lambda \qquad (37)$$

Here B_λ, K'_λ and K_λ are individual terms in the summation of equns (27), (28) and (29). The total ion-size correction of the Hamiltonian matrix element is given by the right hand side of equation (31) with the parameters A_o, J_o' and J_o replaced by A, J' and J. A and B are the lowest order terms formulated by BSG and J and K are the ones introduced by Zwicker. J' and K' are parameters of the same order as J and K, as can be seen from the above definitions (J, K, J' and K' contain an extra r^2 factor in the integrand). The primed parameters were neglected in Zwicker's paper.

Presumably he retained only the lowest order terms that include the s- and p-core interaction, as J and K are the lowest order parameters which contain the overlap with p-cores.

In Table I we present the values of the first two orders of the ion-size parameters for the neutral rare gas atoms Ne, Ar and Kr. The first line gives the parameters of the whole atoms while the next line gives the parameters evaluated excluding the contribution of the outermost s and p shells (minus 8 electrons). The reason for including these will become apparent later.

Table I

	A	B	J	K	J'	K'
Ne	12.63	30.50	27.26	76.82	73.38	96.06
	7.45	.25	-.01	0	1.56	.06
Ar	15.77	93.98	116.51	516.32	171.00	549.84
	26.88	2.55	2.70	.35	16.53	1.53
Kr	17.61	131.49	143.33	841.59	266.07	961.92
	36.87	4.45	6.94	1.22	30.69	3.60

First two order ion-size parameters for Ne, Ar and Kr, as defined in the text. For each atom the first line is for the entire atom and the second line is excluding the outermost s and p shells.

For the slowly varying approximation to work the higher order terms are expected to contribute less and less. The Taylor's series of equn (25) can then be truncated after a few terms without loss of accuracy. Unfortunately we have found that this is not the case. We have evaluated the energies of simple systems such as the Rydberg series in alkali atoms, F-center in NaCl and the self-trapped exciton using the ion-size parameters evaluated including all electrons of the atoms. The energies were in medio-

cre agreement. Also it was sometimes impossible to find the minimum of energy in a variational calculation. A close examination of the Taylor's series terms revealed that the 2nd order terms were larger than the 1st order terms! The problem lies in the fact that the outer shell orbitals are not 'compact' enough compared to the pseudofunction to meet the requirement of the slow varying approximation. If the damping parameter of the pseudofunction gaussian were sufficiently small (a diffuse pseudofunction), the Taylor's series would converge despite the large orbitals. For excited states in rare gas solids of interest the expected optimum damping parameters are not small enough according to studies of various systems.

Fortunately, as is suggested by Table I the deep cores can be well represented by the first two order ion-size parameters. This leads us to conclude that the ion-size theory based on the SVA is satisfactory only in the treatment of deep core orbitals. All bubble calculations reported in this thesis will use the zeroth order expansion terms for the deep core treatment, as the first order terms are relatively small.

I-b) Pseudopotential for outer shell electrons:

In the previous section it is stated that the outer shell of atoms cannot be treated by the SVA efficiently. That is, in principle, the series of equn (25) will eventually converge, but only after a large number of terms. To have a great number of terms to deal with is not our aim. The obvious alternative is simply to treat the outer shell orbitals exactly. We do not intend to evaluate all the integrals exactly as one would do in

the extended ion model. Rather, we will employ the following efficient scheme of interpolation. This scheme relies heavily on the use of 1s-type gaussian as the pseudofunction. A number of exact values of the pseudopotential's various terms are fitted by a set of simple and accurate analytical expressions. The least squares method is used for the fitting. The particular matrix elements chosen for the fit are diagonal elements of gaussians whose damping parameter ranges from .005 to .16 in units of (bohr rad.)-2 and whose distance to the core orbitals ranges from 0 to 15 bohr radii. In the next three subsections we present details of the treatment for the three extended-ion terms.

i) The screened Coulomb potential

The screened Coulomb potential produced by the outermost shell is represented by a single term of the form:

$$V_{sc}(r) \rightarrow \frac{A_1 e^{-\beta_1 r^2}}{r} \qquad (38)$$

where A_1, β_1 are determined by the least square fitting with the exact values of the Coulomb integral for the set of gaussians briefly described above. The matrix element between a pair of gaussians, $e^{-\alpha_1 r_A^2}$ and $e^{-\alpha_2 r_B^2}$, would be:

$$\int e^{-\alpha_1 r_A^2} V_{sc}(\tau) e^{-\alpha_2 r_B^2} d\tau \rightarrow A_1 \int e^{-\alpha_1 r_A^2} \left(\frac{e^{-\beta_1 r_0^2}}{r_0}\right) e^{-\alpha_2 r_B^2} d\tau \qquad (39)$$

$$= A_1 e^{-IR} \frac{2\pi}{(\beta_1+\alpha_1+\alpha_2)} F_0\left[(\beta_1+\alpha_1+\alpha_2)\,|\vec{R}_0 - \vec{R}_m|^2\right], \quad r_0 = |\vec{r} - \vec{R}_0|$$

$$IR = \beta_1 R_0^2 + \alpha_1 R_A^2 + \alpha_2 R_B^2 - \frac{1}{(\beta_1+\alpha_1+\alpha_2)}\left[(\alpha_1 R_{Ax} + \alpha_2 R_{Bx} + \beta_1 R_{0x})^2\right.$$

$$\left. + (\alpha_1 R_{Ay} + \alpha_2 R_{By} + \beta_1 R_{0y})^2 + (\alpha_1 R_{Az} + \alpha_2 R_{Bz} + \beta_1 R_{0z})^2\right],$$

$$\vec{R}_m = \frac{\alpha_1 \vec{R}_A + \alpha_2 \vec{R}_B + \beta_1 \vec{R}_0}{\alpha_1 + \alpha_2 + \beta_1}\ ; \quad F_0(t) = \frac{1}{2}\left(\frac{\pi}{t}\right)^{1/2} \exp(\sqrt{t})$$

The exact values of the Coulomb energy are obtained by numerical integration using the method of multipole expansion (see Appendix A). An example of the fit made for Ne is given in Table II. The range was determined from a preliminary study of typical systems such as atomic Rydberg levels, impurity state in RGS and conduction band in RGS. We must keep in mind that the fitted expression must be accurate in the range that include the gaussians' damping parameter used in these systems. Because of the well-known fact that the product of two gaussian functions is a gaussian centered on another site, the above fit of diagonal elements in fact covers all off-diagonal elements.

Table II

R \ α	0.02	0.04	0.08	0.16
0	.2708(-1)	.7420(-1)	.1980(0)	.5072(0)
	.2700(-1)	.7420(-1)	.1986(0)	.5071(0)
3	.1904(-1)	.3721(-1)	.5234(-1)	.4221(-1)
	.1897(-1)	.3712(-1)	.5223(-1)	.4190(-1)
6	.6622(-2)	.4713(-2)	.1027(-2)	.5274(-4)
	.6580(-2)	.4651(-2)	.0962(-2)	.2702(-4)
9	.1141(-2)	.1533(-3)	.2021(-5)	
	.1127(-2)	.1464(-3)	.1280(-5)	
12	.9746(-4)	.1332(-5)		
	.9533(-4)	.1161(-5)		

Fit of the screened Coulomb energy (without the negative sign) contributed by the 2s and 2p shells of Ne. α is the gaussian damping factor of the pseudofunction and R is the distance between a Ne atom and the site of the pseudofunction. The first and second lines are the exact and fitted values respectively. The integer inside the parentheses is the decimal exponent. All in atomic units.

We tabulated the parameters A_i and β_i for Ne, Ar and Kr in

Table V. As the RMS deviation shows, the fit is very accurate within the range of gaussian used. From Table II it can be seen that with very compact gaussian and large distances, the fit deteriorates. Their contribution, however becomes less important at the same time with increasing R.

ii) The exchange energy

We have evaluated the exchange integrals between a pair of 1s gaussians for the same range of α and R as above. By accurately representing the atomic wavefunctions of Clementi and Roetti by a large number of gaussians, these integrals can be readily evaluated analytically (see Appendix B). Two different forms of interpolation were tried.

The first one could be called the fit of the exchange in exact form. The exchange energies due to the outer s- and p-electrons are calculated separately. For each case, the orbitals are represented by a single s- or p-type gaussian. The expression for the integrals can be determined analytically and fitted to their respective exact values. Unlike the Coulomb integral the quality of agreement for unlike pairs of gaussians (off-diagonal matrix elements) is not garanteed since the exchange energy is a two electron integral and the gaussians are integrated in different coordinates. The gaussian product rule does not apply here as it did for the Coulomb energy. Fortunately, it was found that the off-diagonal matrix elements as calculated from the interpolation formula agrees with the exact values to the same accuracy of the diagonal elements fit.

The second form is referred to as the exchange fit in Sla-

ter form. Here, a 1s gaussian function represents the core charge density. The resulting analytical form is much simpler than those of the previous one. To our great surprise we found this approach giving a slightly better fit than the first one, in spite of the fact that the first one has the non-local form of exchange. Also, the interpolation for the cases of unlike gaussians agrees with the exact values to the same order of accuracy as the fit.

The above two schemes of interpolation of the exchange energy are of comparable accuracy. Finally, we have adopted the Slater form of exchange since it employs simpler expressions.

The interpolation is done as follows:

$$\sum_{\lambda} e^{-\alpha_1 r_{1A}^2} \chi_{\gamma\lambda}(r_2) \frac{1}{r_{12}} \chi_{\gamma\lambda}(r_1) e^{-\alpha_2 r_{2B}^2} d\tau_1 d\tau_2 \qquad (40)$$

$$\rightarrow A_2 \int e^{-\alpha_1 r_A^2} e^{-\beta_2 (\vec{r} - \vec{R}_\gamma)^2} e^{-\alpha_2 r_B^2} d\tau = A_2 \left(\frac{\pi}{\beta_2 + \alpha_1 + \alpha_2} \right)^{3/2} e^{-IR}$$

where the quantity at the left of the arrow is the exact exchange contribution of the outer shell electrons, the parameters A_2 and β_2 are optimized by a least square routine and IR is defined as in the Coulomb integral. The parameters A_2 and β_2 for Ne, Ar and Kr are presented in Table V. It should be emphasized that the exchange energy employed in this pseudopotential is fitted well to the non-local exchange. Also, we are not making the substitution of a non-local operator by a local operator as was done by Slater. It is rather the case of substituting the exact values by an interpolation formula which happens to be of the Slater form. For comparison, we have evaluated the usual Slater exchange defined by the exact charge density in the $X\alpha$ scheme[13]. The Slater exchange appears in Table III. As expected, it overestimates the energy at

large distances especially for compact gaussians.

Table III

R \ α	0.02	0.04	0.08	0.16
0	.4347(-1) .4330(-1) .4345(-1)	.1115(0) .1115(0) .0944(0)	.2647(0) .2654(0) .1845(0)	.5584(0) .5592(0)
3	.3107(-1) .3092(-1) .3269(-1)	.5923(-1) .5922(-1) .5752(-1)	.8452(-1) .8593(-1) .8167(-1)	.7993(-1) .8764(-1)
6	.1135(-1) .1126(-1) .1410(-1)	.8923(-2) .8882(-2) .1414(-1)	.2851(-2) .2917(-2) .1057(-1)	.3226(-3) .3374(-3)
9	.2124(-2) .2092(-2) .3634(-2)	.3880(-3) .3761(-3) .9540(-3)	.1285(-4) .1038(-4) .9072(-3)	
12	.2039(-3) .1981(-3)	.5102(-5) .4495(-5)	.1440(-7) .3875(-8)	

Fit of the exact exchange energy (without the negative sign) contributed by the 2s and 2p shells of Ne. The first and second lines are the exact and fitted values respectively. The third line is the Slater exchange from the same electron shells. All in atomic units.

iii) Overlap integrals

The fits of the overlap integrals are made separately for the s and p orbitals. In the beginning, we have tried to fit the ssσ overlap by the use of a single gaussian:

$$\int e^{-\alpha r_{iA}^2}\, \chi_s(r)\, d\tau \rightarrow N \int e^{-\alpha r_A^2}\, e^{-\beta r^2}\, d\tau \qquad (41)$$

where N is the normalization factor for $e^{-\alpha r^2}$ and β is the parameter to be determined by fitting. The spσ integral is fitted according to

$$\int e^{-\alpha r_{iA}^2}\, \chi_{pz}(r)\, d\tau \rightarrow N' \int e^{-\alpha r_A^2}\, e^{-\beta r^2}\, z\, d\tau \qquad (42)$$

where we take the z-axis along the direction of $\vec{R}_A$, N' is the normalization factor for the p-type gaussian and β is the adju-

Table IV-a

R \ α	0.02	0.04	0.08	0.16
0	.1962(0) .1963(0)	.3119(0) .3119(0)	.4735(0) .4735(0)	.6705(0) .6705(0)
3	.1650(0) .1652(0)	.2234(0) .2234(0)	.2532(0) .2531(0)	.2174(0) .2170(0)
6	.9820(-1) .9834(-1)	.8215(-1) .8229(-1)	.3925(-1) .3943(-1)	.8636(-2) .8842(-2)
9	.4137(-1) .4146(-1)	.1560(-1) .1566(-1)	.1879(-2) .1905(-2)	.7753(-4) .7168(-4)
12	.1235(-1) .1238(-1)	.1544(-2) .1555(-2)	.3227(-4) .3135(-4)	
15	.2613(-2) .2623(-2)	.8106(-4) .8148(-4)		

Fit of the overlap integral (ssσ) between the 2s shell of Ne and a gaussian pseudofunction. The first and second lines are the exact and fitted values respectively. All in atomic units.

stable parameter. We found that these formulas could not make a fit of comparable accuracy as the fit of Coulomb and exchange energies. This indicates that a quantity directly related to the core wavefunctions, such as the overlap, is harder to fit in terms of a single gaussian. We have found that a satisfactory fit is achieved by using pairs of gaussians for both overlaps. The two gaussian damping parameters are related by a simple ratio. A constant factor of 1/4 was found to be reasonable for all atoms studied. In the earlier single gaussian fits we have noticed that the parameters β_{ss} and β_{sp} were very close in value. That is what one might expect as the two core shells belong to the same principal quantum number. Given this, we decided to use the same set of β_{ss} and β_{sp} for both ssσ and spσ. The number of adjustable parame-

Table IV-b

R \ α	0.02	0.04	0.08	0.16
3	.3815(-1) .2650(-1)	.7008(-1) .6796(-1)	.1408(0) .1409(0)	.2062(0) .2113(0)
6	.3399(-1) .3170(-1)	.5392(-1) .5082(-1)	.4960(-1) .4588(-1)	.2295(-1) .1889(-1)
9	.2203(-1) .2019(-1)	.1674(-1) .1488(-1)	.4822(-2) .3568(-2)	.7413(-3) .2511(-3)
12	.9101(-2) .8128(-2)	.2558(-2) .2040(-2)	.2043(-3) .0847(-3)	.1717(-4) .0062(-4)
15	.2538(-2) .2181(-2)	.2139(-3) .1395(-3)		

Fit of the overlap integral $(sp\sigma)$ between the 2p shell of Ne and a gaussian pseudofunction. The first and second lines are the exact and fitted values respectively. For R = 0, the overlap integral is identically zero. All in atomic units.

Table V

	Screened Coulomb			Exchange		
	β_1	A_1	RMSD	β_2	A_2	RMSD
Ne	1.3264	-4.0871	.1x10-3	.5776	-2.6268	.1x10-2
Ar	.6672	-5.3569	.4x10-3	.2275	-1.5550	.5X10-2
*Kr	.5120	-5.5420	.2x10-3	.1850	-1.4291	.2x10-2
	$(ss\sigma)$			$(sp\sigma)$		
	β_3	A_S	RMSD	β_3	A_p	RMSD
Ne	1.04	0.2482	.2x10-3	1.04	0.2490	.2x10-2
Ar	0.58	0.3852	.3x10-2	0.58	0.4536	.1X10-2
*Kr	0.52	0.5328	.8x10-3	0.52	0.6387	.4x10-3

Pseudopotential parameters which fit the exact values of the various terms of the Hamiltonian within the range of α (0.005 to 0.16 a_o^{-2}) and R (0 to 15 a_o). Also shown are the root mean square deviations (RMSD) of the fit for each term. All in atomic units. The sign * indicates that the range of α is 0.005 to 0.08 a_o^{-2}.

ters have increased from two in the single gaussian scheme to

three in the double gaussian scheme:

$$\chi_s \rightarrow N\left[N_1 e^{-\beta_3 r^2} + A_s N_2 e^{-\beta_3 r^2/4}\right] \qquad (43)$$

$$\chi_p \rightarrow N'\left[N_1' e^{-\beta_3 r^2} + A_p N_2' e^{-\beta_3 r^2/4}\right] \cdot z \qquad (44)$$

where N_1, N_2, N_1', N_2' are the normalization constants of the individual gaussians and N, N' are the normalization factors of the combined functions. The parameters A_s, A_p and β_3 are listed in Table V. Examples of the overlap integrals for Ne are shown in Tables IVa) and IVb).

In summary to the interpolation formula section, we must restate that it is important to have the three pseudopotential terms fitted to sufficient precision. The overlap energy term is about of equal magnitude of the sum of the Coulomb and exchange terms and is of opposite sign. For typical pairs of gaussians the sum of the three terms comes to about a few percent in absolute value of the individual terms. The accuracy in absolute value is of the same order as the individual fits, but percentage-wise it has become more or less mediocre. Since the electron bubble problem usually employs gaussians centered at the origin (where there is no atom) and atoms at least eight bohr radii distant, the total of the ion-size contribution are small compared to the kinetic energy. It is not that the ion-size terms are unimportant (after all, they create the bubble); a change of 5%, say, of the ion-size terms will not change the bubble drastically. A change of that magnitude increases the first shell displacement by .02 bohr raduis and that of the fourth shell, by .01 bohr radius. The total energy of the system increases by .0005 hartree which comes to about 1% of the energy. This probably means that the ion-size

correction constitutes about 20% of the total energy. The amount by which the bubble radius increased is primarily determined by the rate of change of the ion-size terms with respect to the distance between the gaussians and the atoms. Since these term behave almost as an exponential function of the distance, the rate of change is approximately proportional to the value of the terms themselves, thus making the rate of change relatively small. It is not surprising that an increase of 5% for the rate doesn't change the bubble very much.

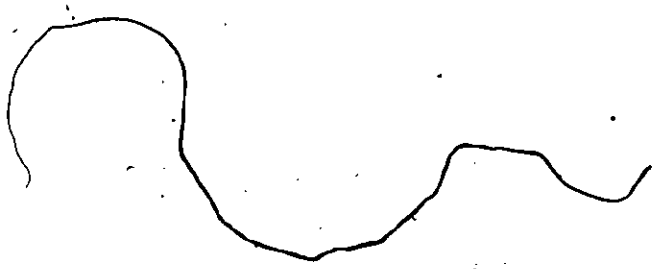

Table VI

Ion-Size Terms for Outer Shell of Neon

Exact Values

R	.02	.04	.08
0	-.07055	-.18566	-.46284
	.07427	.18778	.43352
	.00373	.00212	-.02932
6	-.01798	-.01364	-.00388
	.01960	.01550	.00507
	.00162	.00186	.00119

Values from Interpolation

R	.02	.04	.08
0	-.07030	-.18566	-.46397
	.07436	.18769	.43257
	.00406	.00203	-.03140
6	-.01784	-.01353	-.00388
	.01951	.01516	.00479
	.00167	.00173	.00091

Diagonal elements of the ion-size terms for Ne. The first line is the sum of the Coulomb and exchange energies. The second one is the overlap energy which is almost equal in magnitude to the Coulomb and exchange integrals. The total ion-size term of a diagonal element appears in the third line. The corresponding attractive terms and repulsive terms from the exact value table and the interpolated value table agree very well as indicated by the root mean square deviations of the individual fits in Tables II, III, IVa) and IVb). However when everything is summed together there is a loss of accurate significant figures for the total.

Section II Polarization Energy

The system of the electron bubble has a net charge of -e. This means that polarization effects will take on an important role in the problem. Polarization, being a minor player in most

defect calculations, is usually subject to rough approximations and assumptions. In an attempt to treat polarization as accurately as possible, we have adopted the Mott-Littleton method[14]. Here we assume that all atoms behave as point dipoles whose polarizability is the free atomic polarizability. This is valid when the overlap between neighbouring atoms is small. Unfortunately, large displacements do occur in the electron bubble, and some pairs of atoms get 16% closer than they were in the perfect crystal. Since there is no simple way of estimating the effect of these situations on the polarizability value, it will be left unchanged.

Table VII

	Polarizability
Ne	2.646
Ar	10.893
Kr	16.441

Table listing the atomic polarizability of the three elements of interest in this thesis. The source is reference 15. In atomic units.

Another approximation is that all dipole vectors and electric field vectors are constrained to be radial. We consider this reasonable because the electron charge cloud and the atomic displacements are of radial symmetry. This also make the computations easier.

The method is the following. The dipole moment of an atom at site $\vec{R}_\gamma$ is :

$$\vec{\mu}(\vec{R}_\gamma) = \alpha \vec{E}(\vec{R}_\gamma) \qquad (45)$$

where $\vec{\mu}$ is the dipole moment, α is the atomic polarizability and

$\vec{E}$ is the local electric field. Note that we get $\vec{R}_\gamma$, $\vec{\mu}$ and $\vec{E}$ parallel. We divide the lattice in two parts. In one part, the point dipoles are far enough from the source that the local electric field can be calculated with negligeable error from continuum considerations.

$$\vec{\mu}(R_\gamma) = \frac{a^3}{4}\frac{Q}{4\pi}\left(1 - \frac{1}{K_0}\right)\frac{\hat{R}_\gamma}{R_\gamma^2} \qquad (46)$$

where Q is the charge enclosed in a sphere of radius R_γ. Here R_γ is large enough and Q = -1.(atomic units) K_0 is the dielectric constant determined from the Clausius-Mosoti equation:

$$\alpha = \frac{3}{4\pi}\left(\frac{a^3}{4}\right)\frac{K_0 - 1}{K_0 + 2} \qquad (47)$$

The extra 1/4 comes from the fact that there is 4 atoms per unit cell in the FCC structure of RGS. In the other part, the dipole moments are left unknown and are determined self-consistently in the discrete model.

$$\vec{\mu}(\vec{R}_\gamma) = \alpha(\vec{E}_1 + \vec{E}_2 + \vec{E}_3) \qquad (48)$$

where $\vec{E}_1$ is the electric field due to the defect electron, $\vec{E}_2$, the electric field due to the dipoles contained in the part of the lattice where they are determined self-consistently and $\vec{E}_3$, the electric field to the dipoles that are determined from the continuum approximation.

Some details concerning the three contributions of local electric field:

1) $\vec{E}_1$ of defect electron: The electric field due to a spherically symmetric cloud of charge is

$$\vec{E}(\vec{R}_\gamma) = Q_\gamma \frac{\hat{R}_\gamma}{R_\gamma^2} \qquad (49)$$

where Q is the charge enclosed inside a sphere of radius R_γ. The

charge density of the defect electron is just the magnitude squared of the wavefunction. This wavefunction is not necessarily spherically symmetric since it must be orthogonal to all the core orbitals of the surrounding atoms. To take into account the oscillations of the charge density present at the core sites, we do as follows. Write out the density for the wavefunction Ψ.

$$\rho = |\Psi|^2 = N^{-2}\left[|\phi|^2 - 2\sum_{\gamma\lambda}\langle\phi|\chi_{\gamma\lambda}\rangle\chi_{\gamma\lambda}\phi + \sum_{\gamma\lambda}\sum_{\gamma'\lambda'}\langle\phi|\chi_{\gamma\lambda}\rangle\langle\chi_{\gamma'\lambda'}|\phi\rangle\chi_{\gamma\lambda}\chi_{\gamma'\lambda'}\right] \tag{50}$$

The electric field is

$$\vec{E}_1(\vec{r}) = \int d\vec{r}' \frac{(\vec{r}' - \vec{r})}{|\vec{r}' - \vec{r}|^3}|\Psi|^2 \tag{51}$$

The first term is

$$\hat{r}\frac{N^{-2}}{r^2}\int_0^r d\vec{r}'\,|\phi|^2$$

For the other terms, we approximate the factor $\frac{\vec{r}' - \vec{r}}{|\vec{r}' - \vec{r}|^3}$ in the integrand as being constant over the range of the core orbitals $\chi_{\gamma\lambda}$ and $\chi_{\gamma'\lambda'}$. Using the fact that $\langle\chi_{\gamma\lambda}|\chi_{\gamma'\lambda'}\rangle = \delta_{\lambda\lambda'}\delta_{\gamma\gamma'}$ we get

$$\vec{E}_1(\vec{r}) = \frac{\hat{r}}{r^2}N^{-2}\int_0^r d\vec{r}'\,|\phi|^2 - \sum_{\gamma\lambda}|\langle\phi|\chi_{\gamma\lambda}\rangle|^2 N^{-2}\frac{(\vec{R}_\gamma - \vec{r})}{|\vec{R}_\gamma - \vec{r}|^3} \tag{52}$$

In earlier works, the first term is usually used as an approximation for $\vec{E}$. The second term is a correction term due to the orthogonality requirement of the wavefunction. Details about the overlap integral are given in the previous section. Note that when we put $\frac{\vec{r}' - \vec{r}}{|\vec{r}' - \vec{r}|} \to \frac{\vec{R}_\gamma - \vec{r}}{|\vec{R}_\gamma - \vec{r}|}$, we effectively 'squash' all density variation into a point contact term. This way, only monopolar corrections are included in $\vec{E}_1$. The dipolar terms, which arises mostly from orthogonalization with p-core orbitals are neglected.

In all the bubble calculations reported in this thesis, three gaussians pseudo-functions were placed at the origin, the vacancy site. The bases coefficients calculated by the diagonalization of the electron Hamiltonian were used in determining the charge density. Say that we had

$$\Psi = c_1\Psi_1 + c_2\Psi_2 + c_3\Psi_3 \qquad (53)$$

and $$\Psi_i = \phi_i - \sum_{\gamma\lambda} \langle \phi_i | \chi_{\gamma\lambda} \rangle \chi_{\gamma\lambda}$$

where Ψ_i are the bases and c_i are the coefficients.

$$\rho = c_1^2\Psi_1^2 + c_2\Psi_2^2 + c_3\Psi_3^2 + 2c_1c_2\Psi_1\Psi_2 + 2c_2c_3\Psi_2\Psi_3 + 2c_1c_3\Psi_1\Psi_3 \qquad (54)$$

The squared terms are identical with the previous expression (equn 52). The cross-term is :

$$\Psi_1\Psi_2 = \frac{\hat{r}}{r^2} N_1^{-1} N_2^{-1} \int_0^r d\vec{r}' \; \phi_1(r')\,\phi_2(r') - N_1^{-1}N_2^{-1} \sum_{\gamma\lambda} \langle \phi_1 | \chi_{\gamma\lambda} \rangle \langle \chi_{\gamma\lambda} | \phi_2 \rangle \frac{(\vec{R}_\gamma - \vec{r})}{|\vec{R}_\gamma - \vec{r}|} \qquad (55)$$

2) Field produced by dipoles: The field produced at site r_n by many dipole moments is:

$$E_2(r_n) = \sum_m \frac{3(\mu_m \cdot r_{mn})\,\vec{r}_{mn} \cdot \vec{r}_n - r_{mn}^2\,\vec{\mu}_m \cdot \vec{r}_n}{r_{mn}^5} \qquad (56)$$

where $\vec{r}_{mn} = \vec{r}_m - \vec{r}_n$

and where the summation excludes the site m for which $\vec{r}_{mm} = 0$. This exception applies for all subsequent summations over dipole sites. Knowing that the $\vec{\mu}$'s belonging to the same shell are equal in magnitude, this summation can be reduced to a summation over shells. This results in the equations

$$\mu_i = \alpha \left(E_1(r_i) + \sum (SS)_{ij}\,\mu_j \right) \qquad (57)$$

where the set of numbers SS_{ij} are special shell summations which

depend on the radius vectors of sites in shells i and j. The electric field contribution of the exterior region where the dipole values are calculated from the continuum model can be of relatively small effect if the inner region is made up of a large number of shells. Thirteen shell for the inner lattice was found to be large enough so that the exterior region's dipoles can be ignored. More details are given in Appendix E. The above 13 simultaneous equations can be solved by the standard matrix method. Though a 13 X 13 matrix can easily be inverted by computer subroutine, it was decided to use an iterative method to save computer time (these equation have to be solved about a thousand times in the course of a computation since new coefficients SS_{ij} are calculated every time a shell undergoes a displacement). The iterative method is very simple. The initial values of μ_i is estimated from the continuum values:

$$\mu_i = \frac{a^3}{4} \frac{Q}{4\pi} \left(1 - \frac{1}{k_0}\right) \frac{\hat{r}_i}{r_i^2} \qquad (46)$$

Inserting this set of μ_i into equn (57), new μ_i's are obtained. This process is repeated four times to assure a good convergence of at least four figures.

Once all dipole moments are known, we obtain the polarization energy expressed in terms of monopole-dipole and dipole-dipole interaction:

$$E_{pol} = -\frac{1}{2} \sum_{\vec{r}_i} \vec{E}_{1oc}(\vec{r}_i) \cdot \vec{\mu}(\vec{r}_i) + \text{dipole-dipole interaction} \qquad (58)$$

which becomes simply

$$E_{pol} = -\frac{1}{2} \sum_{\vec{r}_i} \vec{E}_i(\vec{r}_i) \cdot \vec{\mu}(\vec{r}_i) \qquad (59)$$

as shown in Druger and Knox[16]. When $j > 14$, the electric field is

like the one produced by a point charge at the origin and the dipole moment is given by the continuum approximation. This part of the sum goes simply as $1/r^4$, and creates no problem at all in the evaluation:

$$E_{pol} = -\frac{1}{2}\sum_{i}^{12} E_{ii}\,\mu_i\,no_i - \frac{a^3}{4}\frac{1}{4\pi}\left(1-\frac{1}{k_o}\right)20.467\,a^{-4} \qquad (60)$$

where no_i is the number of atoms in shell i.

Section III Interatomic potential

The rare gas solid is usually treated as a collection of atoms interacting pairwise. In this work we use the 6-12 type potential for Ne, Ar and Kr as presented in Kittel[17]. Although other types of potential are available, we decided it would be better to use the potential type which is readily available for all three atoms.

One must be careful in the choice of interatomic potenital. In the case where the lattice is greatly compressed in the neighborhood of the bubble, the hard core portion of the potential is of particular importance. Since the $1/r^{12}$ part of the 6-12 potential is the least reliable part, its use may be questioned.

This problem was examined in some detail. We performed two static (i.e. no kinetic energy contribution to the lattice) bubble calculation for Ne solid, once using the 6-12 potential, and again using a more accurate one proposed by Aziz[18]. Because both are derived from properties of gas, it could be said that both are equivalently valid (or at most, equivalently uncertain) in dealing with atoms interacting in solids.

As we can see in the above Table VIII, that the Aziz potential

Table VIII

	6-12	Aziz
displacement of first shell	2.43	2.31
total energy of system	.0519	.0540

Table comparing the effect of different potential in static bubble calculation in solid Ne. Thirteen shells are allowed to displace. All in atomic units.

which has a stiffer core allows slightly less compression of the latice than does the 6-12 potential. Most of the difference in total energy reflects the fact that the neighboring atoms being closer, the ion-size terms of the electronic Hamiltonian increases. If the exact interaction potential of atoms in the solid were known and were used in our calculation, we would expect that the difference in total energy with respect to either of the two listed above will be of the same order as the difference of the two. Consequentially, an uncertainty of .002 Hartree is attached to subsequent bubble calculations in Ne. In the other solids, the displacements of atoms are substantially smaller. The pair separation of the nearest neighbors are closer to normal, thus making the deformation energy more reliable.

The 6-12 potential is written in the form:

$$v(r) = 4\varepsilon\left[\left(\frac{\sigma}{r}\right)^{12} - \left(\frac{\sigma}{r}\right)^{6}\right] \qquad (61)$$

where the parameters σ and ε are listed in the table below.

The Aziz potential for Ne is:

$$v(r) = \varepsilon\left[\frac{6}{n-6}\left(\frac{\sigma}{r}\right)^{n} - \frac{n}{n-6}\left(\frac{\sigma}{r}\right)^{6}\right] \qquad (62)$$

Table IX

	Ne	Ar	Kr
$\frac{\varepsilon}{\sigma}$ (10^{-4})	1.147 5.178	3.837 6.425	5.147 6.898

Values of the 6-12 potential parameters for the rare gases taken from Kittel (ref. 17).

$$n = 13 + \gamma((\sigma/r)^{-1} - 1)$$

where the constants are

$$\gamma = 5$$
$$\sigma = 5.8088\ a_0$$
$$\varepsilon = 1.305 \cdot 10^{-4}\ Hr$$

III.a) Lattice model

In a discrete lattice model, the deformation energy is defined as the difference of interatomic potential energy plus the difference of kinetic energy effects (lattice free energy) between a given lattice configuration and the perfect lattice. The difference in kinetic energy can be neglected for solids of heavier atoms (Ar and Kr). An approximate scheme was devised to take into account the kinetic energy in solid Ne at different temperatures. We will go into some detail in a later subsection.

Our model consists of 13 displaceable shells totalling 248 atoms while the rest of the lattice is 'frozen'. Each atom of the inner shells interacts with its 134 closest neighbors which can include the frozen atom outside the 13th shells. 134 atoms corresponds to 7 shells, the last one having a radius of about twice the lattice parameter. In principle, we can extend the range of

the potential further. Since we detected no significant change in bubble size when the range was enlarged, we opted to fix the range at 134 atoms. Also, it was deemed practical to constrain the atoms to displace radialy. This way the polarization and the deformation calculation becomes completely compatible. Shells defined by at least two symmetry coordinates do not actually move in a radial direction (among the first 13 shells they are (211), (310), (321), (411), (420), (332) and (422)). For instance when the coordinates of an atom in shell (221) change, it is mainly due to the push of the atoms of shell 110 and 200 moving outwards. The excess electron has a small effect at that distance. Now, the atoms of shells 110 and 200 lie in mirror planes containing the origin. This remains true even after the correct lattice relaxation has occured. The atom on site 211 does not lie on a mirror plane similar to the ones of atoms of shells 110 and 200. The geometry of the contacts between that atom and the neighboring atoms belonging to the first two shells is such that atom 221 will be pushed along a direction not necessarily the radial direction. The new coordinates of the (221) shell atoms will be a permutation of the numbers $(2+\delta_1)$ $(1+\delta_2)$ and $(1+\delta_2)$. The values of δ_1 and δ_2 are unrelated in general. The approximation of radial displacements for all shells proposes, in particular, that $\delta_2 = 2*\delta_1$ for shell 211. Similar conditions are implied for the other shells. Bieng a fully consistent system, the approximtaion must have an effect on the shells of single symmetry coordinate (they are (110), (200), (220), (222), (330) and (400)). This effect is expected to be small because the radial approximation is reasonable.

III.b) Minimization method

Only a few comments are required concerning the minimization method. The direct method is used: one system parameter is varied at a time, the parameters being the radial atomic displacements. Other methods are available but require the evaluation of function gradients and possibly second derivatives. For these methods to converge correctly to the equilibrium configuration, the initial displacement values must be very close to the final values, otherwise the second derivative matrix would not be positive definite and the method would become invalid.

The shells which contain atoms along the (1$\bar{1}$0) direction are coupled very strongly with each other. To assure a faster convergence to equilibrium the (110), (220) and (330) shells are the first one to move and the others follow in order of incresing radius. Starting from a perfect lattice where all displacements are zero, the Ne electron bubble reaches equilibrium in about 15 iterations, that is, 15 cycles of optimization of the 13 shells in the order given above. Equilibrium is attained when the change in the first shell displacement is smaller than .01 bohr rad. in consecutive iterations.

Section IV Lattice Free Energy

This section can easily be included as a subsection in the deformation energy section. Although this facet of the electron bubble problem applies only to Ne solid, much attention was devoted to it. What is about to be presented below is a very crude scheme to take into account the changes in vibrational energy of the atoms due to the changes of their local configura-

tion. The underlying idea is that when a particular atom's neighbors get closer, atomic force constants increases thus raising the atom's Einstein proper frequencies and at the same time, the vibration energy. Another way of looking at this is to imagine a particle confined in a box or cell. From the uncertaintv principle, as the cell decrease in volume the 'zero-point' momentum or energy increases. The analogy to the crystal is that the twelve nearest neighbors around an atom serves as the confining walls which the atom cannot pass through.

We shall use the Einstein model of atoms behaving as harmonic oscillators. Each oscillator has a private frequency determined by the curvature of the potential well produced by the surrounding atoms fixed at their average postions. In a perfect crystal all atoms have the same frequency. Around a defect the atoms belonging to the same shell would have the same frequencv. We also take the oscillations as being isotropic (i.e. the three degrees of freedom for each oscillator are identical). This concerns the compressed first shell atoms the most, for the oscillation in the (110) direction is supposed to be stiffer than the ones of the two other directions. We are not bothered in adding this approximation, for this is as gross an approximation as the Einstein model is.

The temperature has an important role to play in the lattice vibrations. The energy of the oscillators will be apropriately expressed in terms of Helmholtz free energy. From now on, it is the vibrational free energy that will be minimized instead of simplv the kinetic energy which is only a part of the free

energy. The free energy of an atom positioned at site i is

$$F_i = \frac{1}{2}\sum v(R) + 3kT \ln\left[2\sinh\left(\frac{\theta_i}{2T}\right)\right] \qquad (63)$$

where $\sum v(R)$ is the energy due to the pairwise potential. θ_i is the Einstein frequency of each of the degrees of freedom for atom i. θ_i is in turn expressed as a function of the average, $\bar{R}_{nn}$, of the nearest neighbor distances :

$$\theta_i = c_0 + c_1(a_{loc} - a) + c_2(a_{loc} - a)^2 \qquad (64)$$

where a is the lattice parameter at temperature T. The c_0, c_1 and c_2 are parameters fitted to various properties of the solid Ne. These may vary with temprature. a_{loc} is the local lattice parameter ($R_{nn} = a_{loc}/\sqrt{2}$). This type of expansion in terms of local lattice parameter connects the oscillator's frequency directly with the immediate environment. Also, this puts the change in free energy as a function of the 13 shell displacements. There is no additional variables to the bubble problem. For a given lattice configuration, each atom of the first 13 shells has a free energy relative to that of the perfect lattice:

$$\Delta F = \left[\frac{1}{2}\sum v(R) - \frac{1}{2}\sum v(R^0)\right] + 3kT\left[\ln\left[2\sinh\left(\frac{\theta}{2T}\right)\right] - \ln\left[2\sinh\left(\frac{c_0}{2T}\right)\right]\right] \qquad (65)$$

where R^0 denotes the perfect lattice sites and c_0 is the perfect lattice frequency. The atoms outside the 13 shells fall into two categories. In one, the atoms are in direct contact with atoms of the 13 shells such that both the changes in interatomic potential and in vibrational free energy are calculated. In the other, only the interatomic potential energy is affected.

The parameters c_0, c_1 and c_2 are fitted as follows. In the

perfect lattice, the local lattice parameter is uniform. Thus all θ are equal to c_o. The free energy of each atom is then

$$F_o = \frac{1}{2}\sum \tilde{\nu}(R^o) + 3kT \ln\left[2\sinh(c_o/2T)\right] \qquad (66)$$

We use the experimental latent heat of sublimation as the value of f_o since it is defined as $-L = \partial F/\partial N = F/N = F_o$ (67)

c_o is solved using the inverse function of sinh:

$$c_o = 2T \ln\left[\frac{x + (x^2+4)^{1/2}}{2}\right] \qquad (68)$$

$$x = \exp\left[\frac{1}{3kT}\left(F_o - \frac{1}{2}\sum \nu(R)\right)\right]$$

when T=0,

$$c_o = \frac{2}{3k}\left(F_o - \frac{1}{2}\sum \nu(R)\right). \qquad (69)$$

c_1 is fitted using the fact that $\partial F/\partial V = 0$ (pressure at equilibrium is negligeable). Since $V = N a^3/4$, we then obtain the condition $(\partial F/\partial a)_{a=a_T} = 0$ (70)

$$\left.\frac{\partial F}{\partial a}\right|_{a=a_T} = \frac{1}{2}\sum \left.\frac{d\nu(R)}{da}\right|_{a=a_T} + \frac{3k}{2}\left[\coth\left(\frac{\theta}{2T}\right)\right]\left.\frac{\partial \theta}{\partial a}\right|_{a=a_T} \qquad (71)$$

$$c_1 = \left.\frac{\partial \theta}{\partial a}\right|_{a=a_T} = -\frac{2}{3k}\left[\tanh\left(\frac{c_o}{2T}\right)\right]\left[\frac{1}{2}\sum \left.\frac{\partial \nu}{\partial a}\right|_{a=a_T}\right] \qquad (72)$$

The derivative of the potential can be easily determined. First,

$$\frac{1}{2}\sum \nu(R^o) = 2\varepsilon\left[A_{12}\left(\frac{\sigma}{R_{nn}}\right)^{12} - A_6\left(\frac{\sigma}{R_{nn}}\right)^6\right] \qquad (73)$$

where A_{12} and A_6 are lattice sums of the type

$$A_n = \sum_{R\neq o} \frac{1}{\alpha(R)^n} \qquad (74)$$

and $\alpha(R)$ is the ratio of the magnitude of the Bravais lattice vector to the nearest neighbor separation. We have $A_6 = 14.45$ and $A_{12} = 12.13$.

$$\therefore \frac{1}{2}\sum \frac{d\nu}{da}\Big|_{a=a_T} = 2\varepsilon\left[-768 A_{12}\frac{\sigma^{12}}{a_T^{13}} + 48 A_6 \frac{\sigma^6}{a_T^7}\right] \quad (75)$$

The third parameter is related to the bulk modulus K_T^{-1} in the following way:

$$K_T^{-1} = V\frac{\partial^2 F}{\partial V^2} = \frac{4}{9a}\left(\frac{d^2}{da^2} - \frac{2}{a}\frac{d}{da}\right) F\Big|_{a=a_T} \quad (76)$$

but $$\frac{df}{da}\Big|_{a=a_T} = 0 \quad (70)$$

$$\therefore K_T^{-1} = \frac{4}{9a_T}\frac{d^2 f}{da^2}\Big|_{a=a_T} = \frac{4}{9a_T}\left[\frac{1}{2}\sum \frac{d^2\nu}{da^2}\Big|_{a=a_T} + \frac{3k}{2}\left[\frac{1}{2T}\left(\frac{d\theta}{da}\Big|_{a=a_T}\right)^2 \cdot \frac{1}{\sinh^2(\theta/2T)} + \coth\left(\frac{\theta}{2T}\right)\frac{d^2\theta}{da^2}\Big|_{a=a_T}\right]\right] \quad (77)$$

and

$$c_2 = \frac{1}{2}\frac{d^2\theta}{da^2}\Big|_{a=a_T} = \frac{1}{2}\tanh\left(\frac{\theta}{2T}\right)\left\{\frac{2}{3k}\left[\frac{9a_T}{4}K_T^{-1} - \frac{1}{2}\sum \frac{d^2\nu}{da^2}\Big|_{a=a_T}\right] - \frac{c_1^2}{2T\sinh^2(\theta/2T)}\right\} \quad (78)$$

For $T = 0K$, $$c_2 = \frac{1}{3k}\left[\frac{9a_T}{4}K_T^{-1} - \frac{1}{2}\sum \frac{d^2\nu}{da^2}\Big|_{a=a_T}\right] \quad (79)$$

and $$\frac{1}{2}\sum \frac{d^2\nu}{da^2}\Big|_{a=a_T} = 2\varepsilon\left[9984 A_{12}\frac{\sigma^{12}}{a_T^{14}} - 336 A_6 \frac{\sigma^6}{a^8}\right] \quad (80)$$

The experimental data and the parameter used in the kinetic energy treatment of solid Ne are given in Table X.

It is difficult to attach physical significance to the temperature dependency of the expansion coefficients. For example, why does c_0 decrease as the temperature increase? On one hand, each oscillator vibrates more vigorously as the temperature rises, or on the other hand the lattice spacing increases thus

Table X

	T = 0 K	T = 24 K(tr. pt)
Sublimation Energy	226 K	255 K
Bulk Modulus (K_T^{-1})	11.2 10 dv/cm^2	6.17 10 dy/cm^2
c_0	40.63 K	30.51 K
c_1	-59.74 K/a_0	-35.98 K/a_0
c_2	46.64 K/a_0^2	3.0 K/a_0^2

Table of experimental data and frequency expansion coefficients of solid Ne. The sublimation energy data is from ref. 19 and the Bulk Modulus is from ref. 20. At T = 24K, the bulk modulus according to the table on page 800 of ref. 20 extrapolates to a very small value such that the constant c_2 become negative. At the triple point temperature, the crystal is very soft indeed. The value of bulk modulus at 20K was adopted as the one for 24K because it was the lowest value listed in the table and because it gave a positive c_2, though it does not make the expansion of theta any more reliable for the first three shell atoms (see text). a_0 is the Bohr radius. To convert °K units into Hartree unit multiply by 3.16816 10-6.

slightly reducing the force constants and the oscillator frequency. The misunderstanding stems from the fact that kinetic energy and free energy are two different things. As kinetic energy may increase, so does the entropy which helps reducing the free energy. Our formalism is based completely on the changes of oscillator free energy rather than changes in vibration internal energy.

One word about the inclusion of the quadratic term for θ. It was made necessary because without it the θ would become negative at relatively small positive changes in local lattice parameter. At T = 0 K, the coefficient c_2 is large enough to

avoid this, but at T = 24 K, it is too small, and the frequency becomes negative quickly. The expansion seems to break-down only for the first three shells near the defect where the local lattice parameter can be one bohr radius greater than in the normal lattice. Presently, we have no simple way of dealing with the oscillator energy for these atoms. Rather than guessing the behavior of these compressed atoms, we simply neglected to account for the free energy changes and included only the pair interaction energy. Table XI presents three cases which shows the effect of including the change in crystal free energy (at T = 0 K, it is sometimes referred to as the zero-point energy change). It is found that neglecting this effect for all atoms 'softens' the crystal: the bubble is larger and the total energy is smaller. The lattice energy is also the smallest among the three. Dropping the zero-point energy change for only the first three shells apparently does not change the bubble size significantly. The difference in d_i for #2 and #3 is .04 a_o while the difference between #1 and #3 is .12 a_o. The jump in lattice energy from cases #2 to case #3 is due to the fact that the zero-point energy calculatin of the first shells of case #2 is simply inaccurate.

It is worth mentioning a calculation of vacancy free energies in rare gas solids by Glyde[21]. He uses a self-consistent harmonic approximation of the Einstein oscillator surrounding the defect. The potential used is a Morse potential which is reliable only near the minimum. For a vacancy calculation this is correct since the displacements are small. The free energy of the system is minimized with respect to the shell displacements and also with respect to the Einstein frequency of the oscillators. Here the

Table XI

Ne bubble at T = 0 K

	#1	#2	#3
d_1	2.43	2.27	2.31
d_2	1.22	.79	.76
d_3	.85	.63	.62
d_4	1.54	1.42	1.44
d_{10}	.72	.67	.68
1 - 4	.89	.85	.87
4 -10	.82	.75	.76
10-17	.72	.67	.68
E_{el}	.0554	.0588	.0585
E_{pol}	-.0131	-.0138	-.0138
E_{latt}	.0096	.0107	.0128
E_{tot}	.0519	.0557	.0575

Table which demonstrates the effect of including the crystal free energy. Case #1 is the one where the zero-point change is not taken into account. In case #2 the oscillator free energy treatment is applied to all atoms. Case #3 is considered the less doubtful because the change in zero-point energy is calculated only for shells farther than the third. In all cases the first thirteen shells are allowed to relax. Only a few displacements are listed here. Below the displacement values are the compression values for pairs of strongly coupled shells. E_{el} is the energy of the electron obtained from diagonalizing the Hamiltonian matrix. E_{latt} is the change in lattice energy which include atomic vibration effects. E_{pol} is the polarization energy. The sum of these quantities is the total energy, E_{tot}, of the bubble system. All in atomic units.

atomic displacements and the frequencies are independent variables. This formulation allows the optimization of the potential well in which atoms vibrate. For this complicated approach more variables are needed. There is no doubt that this method is superior to the one presented in this thesis. The reason it wasn't used is that the integrals involved are more difficult for a 6-12 potential than for a Morse potential. We did not attempt to obtain a Morse potential for Ne because it isn't as reliable as

the 6-12 potential in large displacement situations. That is, the hard core of the Morse potential is not as stiff as the 6-12 potential (this is due to the nature of exponential functions), and is finite at r=0.

Section V Results

Below is represented a sample output for the Ne bubble in equilibrium at 0 K showing the shell displacements and some values pertaining to the polarization energy computation.

The first thing to notice is that the displacement of the shells does not follow a 1/r law as would be the case for a continuous elastic medium . In the elastic medium the deformation of an infinitesimal portion of solid depends only on the force exerted by the infinitesimal portions of material surrounding it. The interatomic potential is not involved directly though qualitatively, it acts through the experimental bulk modulus appearing in the elastic theory. To justify the application of this theory to a problem, the characteristic lengths or distances involved must be greater than the atomic spacing. The structure of the crystal would then appear 'smoothed' out. From the atomistic treatment we see that the displacements are damped very quickly as the shell number increases, giving a length parameter of the order of a. This also implies a large compression of the atoms near the defect. The compression is about 15% of the lattice spacing, and this is out of the range of simple elastic theory. Although the rest of the solid outside the first 13 shells can be made to relax according to elastic theory, the energy contribution is considered

Table XII

shell no. i	distance to defect	radial displ.	E_i	E_i^0	μ_i	μ_i^0
1 - (110)	$\sqrt{1/2}$ a	2.31	0.0140	0.0146	0.0343	0.0336
2 - (200)	a	.76	0.0117	0.0118	0.0278	0.0273
3 - (211)	$\sqrt{3/2}$ a	.62	0.0084	0.0083	0.0190	0.0192
4 - (220)	$\sqrt{2}$ a	1.44	0.0056	0.0056	0.0136	0.0129
5 - (310)	$\sqrt{5/2}$ a	.12	0.0055	0.0055	0.0126	0.0127
6 - (222)	$\sqrt{3}$ a	.16	0.0046	0.0046	0.0105	0.0106
7 - (321)	$\sqrt{7/2}$ a	.28	0.0039	0.0039	0.0089	0.0089
8 - (400)	2 a	.02	0.0035	0.0035	0.0080	0.0081
9 - (411)	$\sqrt{9/2}$ a	.04	0.0031	0.0031	0.0072	0.0072
10- (330)	$\sqrt{9/2}$ a	.68	0.0029	0.0029	0.0070	0.0067
11- (420)	$\sqrt{5}$ a	.03	0.0028	0.0028	0.0066	0.0065
12- (332)	$\sqrt{11/2}$ a	.09	0.0025	0.0025	0.0060	0.0058
13- (422)	$\sqrt{6}$ a	.11	0.0023	0.0023	0.0057	0.0053

Sample output of the minimization routine which determines the lattice configuration of the Ne electron bubble in equilibrium at T = 0K. The lattice parameter a for Ne at T = 0 K is 8.435 a_0. The radial dislacement are in bohr radius. Shells further than the 13th are held fixed. The negative signs for the electric field and the dipole moments are dropped. All in atomic units.

too small to be of significance.

The large displacement of the first shell isn't surprising since it is the shell closest to the excess electron. The large displacements of the fourth and tenth shell can be easily understood. Atoms on the three shells mentioned above occupy the sites (110), (220) and (330). An atom in postion (110) has a nearest neighbor in shell (220), and that neighbor, in turn, has a nearest

neighbor in shell (330), and so on for all shell of type (NN0). The vectors joining the pairs of nearest neighbors are purely radial. Consequently, the atoms of the first, fourth and tenth shells are strongly coupled, as can be demonstrated by the above table. The fact that the next strongly coupled shell, (440), is held fixed may affect the results slightly. One expects that allowing the (440) to relax outwards towards the (550) shell, the lattice energy will decrease. At the same time the whole 13 shells will expand a little thus reducing ion-size terms and electronic energy. Below is a table which compares three runs of the same Ne ,T = 0 K bubble program. They each have a different number of directly coupled shells that are allowed to move.

Table XIII

displacement of shells	run no.		
	1	2	3
d_1	1.83 / .94	2.31 / .87	2.40 / .86
d_4	.89 / .89	1.44 / .76	1.55 / .74
d_{10}		.68 / .68	.81 / .50
d_{17}			.30 / .30
lattice energy	.0596	.0575	.0573
total energy	.0095	.0128	.0135

In run #1 the shells 1 to 8 move, keeping shells 10 and 17 rigid. In run #2 shells 1 to 13 are allowed to displace. This is the case for all other bubble calculations in this thesis. The run #3 is the same as #2 except that a single shell, (440), is added. The change in lattice free energy of shells further than the third one is included in these calculations. The number to the left of the slash is the displacement, and the number to the right is the displacement of that shell relative to the next shell's displacement, in other words, the compression between two successive strongly coupled shells. All in atomic units.

As the number of moveable shells increases, the shell displacements obviously become larger. Though the shell displacements for the three cases in Table XIII are significantly different, the compression changes much less. In particular, going from case #2 to case #3, the compression between the first and fourth shells and the one between the fourth and tenth hardly change while their displacements are non-negligeable. In a stability calculation only the energy is important; the accuracy of the cavity size is secondary. The fact that the difference in total energy between cases 2 and 3 is .0002 Hr (.3%) demonstrates that the inclusion of any strongly coupled shells after the (330) shell is unnecessary. In the other solids, the electron resides in a smaller cavity. Furthermore the compression of the shells is dampened more quickly. This indicates that additional moveable shells will have a lesser effect in these cases than in the Ne case.

Table XIV summarizes the bubble calculations for Ne, Ar and Kr.

Some aspects of the polarization results are worth mentioning. Table XII lists quantities related to polarization in the case of Ne at T = 0K. E_i are the electric fields due to the defect electron, and μ_i are the dipole moments used in the actual polarization calculation (see equn 60). E_i° are the electric fields due to a point charge at the origin (i.e. tha vacancy site), and μ_i° are the dipole moments calculated from continuum consideration (0th order M.-L.).

The E_i's agree well with the E_i°'s at almost all distances.

Table XIV

	Ne		Ar		Kr	
	T=0K	T=24K	T=0K	T=83K	T=0K	T=115K
lattice spacing	8.435	8.559	10.037	10.329	10.669	11.023
d_1	2.31	2.57	.74	1.16	.34	.70
d_2	.76	.89	.08	.24	.00	.07
d_3	.62	.70	.22	.37	.09	.21
d_4	1.44	1.64	.33	.59	.12	.31
d_{10}	.68	.79	.11	.22	.04	.10
1 - 4	.87	1.23	.41	.57	.22	.40
4 -10	.76	.85	.22	.37	.09	.21
10-17	.68	.79	.11	.22	.04	.10
E_{el}	.0585	.0537	.0710	.0584	.0786	.0646
E_{pol}	-.0138	-.0127	-.0361	-.0295	-.0481	-.0383
E_{latt}	.0128	.0119	.0055	.0056	.0024	.0030
E_{tot}	.0575	.0529	.0404	.0345	.0329	.0295

The temperatures 24K, 83K and 115K are the triple point temperatures of Ne, Ar and Kr, respectively. The experimental lattice parameters are listed so that one can appreciate the extent of the deformation in some cases. The first thirteen shells are allowed to relax. Only a few displacements are listed here. Below the displacement values are the compression values for pairs of strongly coupled shells. E_{el} is the energy of the electron obtained from diagonalizing the Hamiltonian matrix. E_{latt} is the change in lattice energy which include atomic vibration effects. E_{pol} is the polarization energy. The sum of these quantities is the total energy, E_{tot}, of the bubble system. All in atomic units.

The largest difference occurs for the first shell where the orthogonalization of the wavefunction effect is more pronounced. The μ_i's don't agree as well at large distances. The reason for this is that the outer shell dipole field contribution is neglected. Since the last inner shells are closer to the outer shells these are affected the most. Supposing that the μ_i^0's were the 'true' value of the four last shell dipole moments, the difference in polarization energy is calculated to be 2.10-5 Hr or .2% of the energy, which is obviously negligeable. At smaller distances, the

μ_i's and the μ_i^0's are not very different especially for the first shell where the discrete character of the material should have more effect. This can be attributed to the relatively small polarizability of the Ne atom. The Kr atom, on the other hand, has larger polarizability (see Table VII). A similar table (Table XV) for Kr is presented.

Table XV

shell no. i	E_i	E_i^0	μ_i	μ_i^0
1 - (110)	0.0181	0.0161	0.2290	0.1819
2 - (200)	0.0093	0.0088	0.0916	0.0993
3 - (211)	0.0058	0.0058	0.0633	0.0653
4 - (220)	0.0043	0.0043	0.0555	0.0489
5 - (310)	0.0035	0.0035	0.0380	0.0397
6 - (222)	0.0029	0.0029	0.0333	0.0330
7 - (321)	0.0025	0.0025	0.0283	0.0283
8 - (400)	0.0022	0.0022	0.0231	0.0248
9 - (411)	0.0020	0.0020	0.0219	0.0221
10- (330)	0.0019	0.0019	0.0233	0.0220
11- (420)	0.0018	0.0018	0.0213	0.0199
12- (332)	0.0016	0.0016	0.0198	0.0180
13- (422)	0.0015	0.0015	0.0196	0.0165

Polarization data for Kr electron bubble at T = 0K. Here, the atomic displacements are not listed because they are not at issue. Shells further than the 13th are held fixed. The negative signs for the electric field and the dipole moments are dropped. All in atomic units.

Right away, we see that orthogonalization effects are a

little more important in Kr than in Ne: E_1 and E_1° are different by 10% and E_2 and E_2°, by 5%, compared to 4% and 1%, respectively, for Ne.

There is an obvious difference between μ_i and μ_i° near the defect. There is no doubt it is due to the strength of the dipole field produced by the neighboring atoms. The jump of the dipole moment value at shell 10 is explained in terms of the special coupling between the first, fourth and tenth shell. In these shells the vectors are all aligned in a (110) direction. On average, the field lines of dipoles reduces the magnitude of the local electric field on atoms (hence, $K_o > 1$). In the cases of the three strongly coupled shells, the field lines combine such that they reinforce each others local electric field to some extent. This phenomenon is also observable for the first and fourth shell where the dipoles calculated are substantially larger than the ones from a continuum model.

Chapter III

Band Calculation

In this chapter we propose a way to calculate conduction band states using the same ion-size parameters of the defect calculation. Originally the aim was to evaluate the free conduction electron state with the same Hamiltonian as for the electron bubble state. It turns out that the present approach with floating 1-s basis has very significant potential even in a energy band calculation. Because a pseudopotential is used, we note that only excited states are accessible to the theory. The valence bands are considered flat, which is a good approximation since more precise self-consistent calculations demonstrate rather flat valence bands.

Section I Hybrid Pseudopotential for Extended States

The orthogonalized floating gaussian basis are formed from a Bloch sum:

$$\Phi_i = N^{-1/2} \sum_{\vec{l}} e^{i\vec{k}\cdot\vec{l}} G_i(\vec{r} - \vec{l} - \vec{a}_i) \qquad (81)$$

where G_i is the normalized gaussian of damping parameter α_i and is centered at a_i relative to the center of each unit cell. $\vec{k}$ is the conduction electron wavevector. The $\vec{l}$'s are atomic sites, and $N^{-1/2}$ is the normalization factor of the Bloch sum. This must be made orthogonal to the valence orbitals:

$$\Psi_i = \Phi_i - \sum_{\lambda} \langle X_\lambda | \Phi_i \rangle X_\lambda \qquad (82)$$

where

$$X_\lambda = N^{-1/2} \sum_{\vec{l}} e^{i\vec{k}\cdot\vec{l}} \chi_{l\lambda}(\vec{r}) \quad ; \quad \chi_{l\lambda}(\vec{r}) = \chi_{o\lambda}(\vec{r} - \vec{l}) \qquad (83)$$

The conduction electron energy at wavevector $\vec{k}$ is obtained by

solving the secular determinant:

$$|H_{ij} - E S_{ij}| = 0 \tag{84}$$

where

$$H_{ij} = \langle \Psi_i | H | \Psi_j \rangle \tag{85}$$

$$S_{ij} = \langle \Psi_i | \Psi_j \rangle \tag{86}$$

The hamiltonian matrix element is written out as:

$$H_{ij} = T_{ij} + (V_{sc} + V_{ex})_{ij} - \sum_{\lambda} \varepsilon_{\lambda} \langle \Phi_i | X_{\lambda} \rangle \langle X_{\lambda} | \Phi_j \rangle \tag{87}$$

$$T_{ij} = \langle \Phi_i | -\tfrac{1}{2}\nabla^2 | \Phi_j \rangle \tag{88}$$

$$V_{ij} = \langle \Phi_i | V | \Phi_j \rangle \tag{89}$$

Because the wavefunctions are Bloch sums, all the individual matrix elements will be expressed in terms of a sum and sometimes double sum over lattice sites. For instance, the kinetic energy term becomes:

$$T_{ij} = N \langle \sum_{\vec{l}} e^{-i\vec{k}\cdot\vec{l}} G_i(\vec{r} - \vec{l} - a_i) | T | \sum_{\vec{l}'} e^{i\vec{k}\cdot\vec{l}'} G_j(\vec{r} - \vec{l}' - a_j) \rangle \tag{90}$$

$$= N \sum_{\vec{l}} \sum_{\vec{l}'} e^{-i\vec{k}\cdot\vec{l}} e^{i\vec{k}\cdot\vec{l}'} \langle G_i(\vec{r} - \vec{l} - \vec{a}_i) | T | G_j(\vec{r} - \vec{l}' - \vec{a}_j) \rangle$$

since T operates on the coordinates only. The kinetic energy operator integral is:

$$\langle G_i(\vec{r} - \vec{l} - \vec{a}_i) | T | G_j(\vec{r} - \vec{l}' - \vec{a}_j) \rangle = \left(3 - \frac{2\alpha_i\alpha_j R^2}{(\alpha_i + \alpha_j)}\right) \exp\left(\frac{-\alpha_i\alpha_j R^2}{\alpha_i + \alpha_j}\right)$$

where

$$R^2 = |(\vec{l} + \vec{a}_i) - (\vec{l}' + \vec{a}_j)|^2 \tag{91}$$

The overlap matrix terms is worked out below so that they are expressed in terms of the ion-size parameters and the interpo-

lation formulas when they apply. As in the defect calculation the ion-size parameters are used to treat the deep core orbitals, and the outer shell electrons are treated exactly.

The S matrix element is expanded as so:

$$\langle \Psi_i | \Psi_j \rangle = \langle \Phi_i | \Phi_j \rangle - 2\sum_{\lambda} \langle \Phi_i | X_\lambda \rangle \langle X_\lambda | \Phi_j \rangle + \sum_{\lambda} \sum_{\lambda'} \langle \Phi_i | X_{\lambda'} \rangle \langle X_\lambda | \Phi_j \rangle \langle X_{\lambda'} | X_\lambda \rangle , \tag{92}$$

but

$$\langle X_{\lambda'} | X_\lambda \rangle = \delta_{\lambda' \lambda} . \tag{93}$$

Therefore

$$\langle \Psi_i | \Psi_j \rangle = \langle \Phi_i | \Phi_j \rangle - \sum_{\lambda} \langle \Phi_i | X_\lambda \rangle \langle X_\lambda | \Phi_j \rangle \tag{94}$$

Now

$$\langle \Phi_i | \Phi_j \rangle = N^{-1} \sum_{I} \sum_{\vec{l}'} e^{-i\vec{k}\cdot\vec{I}} e^{i\vec{k}\cdot\vec{I}'} \langle G_i(\vec{r} - \vec{l} - a_i) | G_j(\vec{r} - \vec{l}' - \vec{a}_j) \rangle$$

where $\langle G_i | G_j \rangle = \exp\left(\frac{-\alpha_i \alpha_j}{\alpha_i + \alpha_j} R^2 \right)$ (95)

and where $R^2 = |(\vec{l} + \vec{a}_i) - (\vec{l}' + \vec{a}_j)|^2$.

For outer shells,

$$\langle \Phi_i | X_\lambda \rangle = N^{-1} \sum_{I} e^{-i\vec{k}\cdot\vec{I}} \langle G_i(\vec{r} - \vec{l} - \vec{a}_i) | \sum e^{i\vec{k}\vec{I}'} \chi_{\ell'\lambda}(r) \rangle$$

$$= N^{-1} \sum_{\vec{l}} \sum_{\vec{l}'} e^{-i\vec{k}\cdot(\vec{l} - \vec{l}')} \langle G_i(\vec{r} - \vec{l} - \vec{a}_i) | \chi_{\ell'\lambda}(r) \rangle$$

$$= \sum_{\vec{h}} e^{-i\vec{k}\vec{h}} \langle G_i(\vec{r} - \vec{h} - a_i) | \chi_{o\lambda}(r) \rangle \tag{96}$$

where $\vec{h} = \vec{l} - \vec{l}'$.

When λ = ns, where n is tha value of the principal quantum number of the last shell, the integral is just the ssσ overlap that was

defined in the defect calculation. When $\lambda = np_x$, np_y or np_z, we get the spσ overlap integral as defined earlier multiplied bv the suitable direction cosine. For example $\lambda = np_x$,

$$\langle G_i(\vec{r}-\vec{R}_i) \mid \chi_{o,np_x}(\vec{r})\rangle = SPOV_i(R_i)\frac{R_{ix}}{|\vec{R}_i|} \qquad (97)$$

The np_y and the np_z cases are similar. For inner cores, we make the first order multipole expansion of

$$\langle G_i(\vec{r}-\vec{R}_i)|\chi_{o\lambda}(r)\rangle = \frac{1}{2}F_{io}(o,R_i)\int \chi_{o\lambda}\,d\vec{r} + \frac{1}{4}F_{io}^{(2)}(o,R_i)\int \chi_{o\lambda}\,r^2 d\vec{r}$$

$$+\frac{3}{2}F_{i1}^{(2)}(o,R_i)\left[\frac{R_{ix}}{R_i}\int \chi_{op_x}\,x\,d\vec{r} + \frac{R_{iy}}{R_i}\int \chi_{op_y}\,y\,d\vec{r} + \frac{R_{iz}}{R_i}\int \chi_{op_z}\,z\,d\vec{r}\right] \qquad (98)$$

When λ is an s-state only the two first terms survive while when λ is either a p_x, p_y or a p_z state only one the last three terms remains. This expression is substituted in

$$\sum e^{-i\vec{k}\vec{h}}\langle G_i(\vec{r}-\vec{R}_i)|\chi_{o\lambda}(r)\rangle$$

The above will be multiplied bv a similar term:

$$\sum e^{i\vec{k}\vec{h}}\langle \chi_{o\lambda}(r)\mid G_j(r-R_j)\rangle$$

to form the matrix element $\langle \Phi_i \mid \chi_\lambda\rangle\langle\chi_\lambda\mid \Phi_j\rangle$ and then the summation is made over λ of inner cores.

For λ = s-state,

$$\langle \Phi_i \mid \chi_s\rangle\langle\chi_s\mid\Phi_j\rangle = \left[\sum_{\vec{h}} e^{-i\vec{k}\vec{h}}\left(\frac{1}{2}F_{io}(o,R_i)\int\chi_{o\lambda}\,d\vec{r} + \frac{1}{4}F_{io}^{(2)}(o,R_i)\int\chi_{o\lambda}\,r^2 d\vec{r}\right)\right]$$

$$\left[\sum_{\vec{h}'} e^{i\vec{k}\vec{h}'}\left(\frac{1}{2}F_{jo}(o,R_j)\int\chi_{o\lambda}\,d\vec{r} + \frac{1}{4}F_{jo}^{(2)}(o,R_j)\int\chi_{o\lambda}\,r^2 d\vec{r}\right)\right]$$

$$= \sum_{\vec{h}}\sum_{\vec{h}'} e^{i\vec{k}\cdot(\vec{h}-\vec{h}')}\frac{1}{4}F_{io}(o,R_i)F_{jo}(o,R_j)\left[\int\chi_{o\lambda}\,d\vec{r}\right]^2$$

$$+\sum_{\vec{n}}\sum_{\vec{n}'} e^{-ik(\vec{n}-\vec{n}')}\frac{1}{8}\left(F_{i0}(0,R_i)F^{(2)}_{j0}(0,R_j)+F^{(2)}_{i0}(0,R_i)F_{j0}(0,R_j)\right)\left[\int \chi_{o1}\,d\vec{r}\right]\left[\int \chi_{o1}\,r^2 d\vec{r}\right] \tag{99}$$

For another s-state belonging to the inner core, the factors are the same except for the integral inside the square brackets. The s-states contributions are easily summed together:

$$\sum_s \langle \Phi_i | X_s\rangle\langle X_s|\Phi_j\rangle = \left\{\sum_{\vec{n}} e^{-i\vec{k}\cdot\vec{n}}\frac{1}{2}F_{i0}(0,R_i)\right\}\left\{\sum_{\vec{n}'} e^{i\vec{k}\cdot\vec{n}'}\frac{1}{2}F_{j0}(0,R_j)\right\} B$$
$$+\left[\left\{\sum_{\vec{n}} e^{-i\vec{k}\cdot\vec{n}}\frac{1}{2}F_{i0}(0,R_i)\right\}\left\{\sum_{\vec{n}'} e^{i\vec{k}\cdot\vec{n}'}\frac{1}{4}F^{(2)}_{j0}(0,R_j)\right\}+\right.$$
$$\left.\left\{\sum_{\vec{n}} e^{-i\vec{k}\cdot\vec{n}}\frac{1}{4}F^{(2)}_{i0}(0,R_i)\right\}\left\{\sum_{\vec{n}'} e^{i\vec{k}\cdot\vec{n}'}\frac{1}{2}F_{j0}(0,R_j)\right\}\right]K' \tag{100}$$

where B and K' are the same parameters defined in chapter II.

The p-state contribution becomes a little more complicated since the Bloch sum terms include the direction cosines, different for each lattice sites l or l' , in general. We start by grouping the 3 p-states which belong to the same principal quantum number:

$$\sum_{\alpha=x,y,z}\langle\Phi_i|X_{p\alpha}\rangle\langle X_{p\alpha}|\Phi_j\rangle = \sum_{\vec{n}}\sum_{\vec{n}'} e^{-i\vec{k}(\vec{n}-\vec{n}')}\frac{9}{4}F^{(1)}_{i1}(0,R_i)F^{(1)}_{j1}(0,R_j)$$
$$\left[\left(\int \chi_{op_x}\,x\,d\vec{r}\right)^2\frac{R_{ix}R_{jx}}{R_iR_j}+\left(\int \chi_{op_y}\,y\,d\vec{r}\right)^2\frac{R_{iy}R_{jy}}{R_iR_j}+\left(\int \chi_{op_z}\,z\,d\vec{r}\right)^2\frac{R_{iz}R_{jz}}{R_iR_j}\right] \tag{101}$$

If you wish to add p-states which belong to another principal quantum number, you only need to replace the integral squared by a sum of squared integrals. Since the three np states are equivalent, the expression simplifies to:

$$\sum_{\vec{n}}\sum_{\vec{n}} e^{i\vec{k}(\vec{n}-\vec{n}')}\frac{9}{4}F^{(1)}_{i1}(0,R_i)F^{(1)}_{j1}(0,R_j)\,\hat{R}_i\cdot\hat{R}_j\;K \tag{102}$$

where K is the same parameter defind in chapter II. Because there exists a cross-term in $\vec{n}$ and $\vec{n}'$ implicit in $\vec{R}_i \cdot \vec{R}_j$ ($\vec{R}_i \cdot \vec{R}_j = (\vec{n} + \vec{a}_i)\cdot(\vec{n}' + \vec{a}_j)$), the double sum above cannot be reduced to a product of single sums as was done for s-state contribution.

The matrix element of the short range potential (i.e. the coulomb and exchange combined) is:

$$\langle \phi_i | v | \phi_j \rangle = \langle \Phi_i | \sum_{\ell''} V(\vec{r} - \vec{\ell}'') | \Phi_j \rangle$$

$$= N \langle \Phi_i | V(\vec{r}) | \Phi_j \rangle$$

$$= \sum \sum e^{ik(\ell' - \ell)} \langle G_i(\vec{r} - \vec{\ell} - \vec{a}_i) | V(r) | G_j(\vec{r} - \vec{\ell}' - \vec{a}_j) \rangle \tag{103}$$

The integral can be divided into a deep core part and an outer shell part as in the defect calculation. The deep core contribution is written the same way as in chapter two.

$$\langle G_i(r - R_i) | V(r) | G_j(r - R_j) \rangle = \frac{1}{4} F_{i0}(0, R_i) F_{j0}(0, R_j) A_0$$

$$+ \frac{1}{8}\left[F_{i0}(0, R_i) F_{j0}^{(1)}(0, R_j) + F_{i0}^{(1)}(0, R_i) F_{j0}(0, R_j) \right] J_0'$$

$$+ \frac{9}{4} F_{i1}^{(1)}(0, R_i) F_{j1}^{(1)}(0, R_j) \hat{R}_i \cdot \hat{R}_j J_0 \tag{31}$$

Now we want the term $-\sum_\lambda \varepsilon_\lambda \langle \Phi_i | X_\lambda \rangle \langle X_\lambda | \Phi_j \rangle$ to be incorporated. For the λ = s-state, there is no special difficulty,

$$\left\{ \sum_{\vec{n}} e^{i\vec{k}\vec{n}} \frac{1}{2} F_i(0, R_i) \right\} \left\{ \sum_{\vec{n}'} e^{-i\vec{k}\vec{n}'} F_{j0}(0, R_j) \right\} \sum_s \varepsilon_s \left[\int \chi_{0s} \, d\vec{r} \right]^2 + \cdots$$

For λ = p state, we get a term similar to the overlap:

$$\sum_{\vec{n}} \sum_{\vec{n}'} e^{-i\vec{k}(\vec{n} - \vec{n}')} \frac{9}{4} F_{i1}^{(1)}(0, R_i) F_{j1}^{(1)}(0, R_j) \hat{R}_i \cdot \hat{R}_j \sum_p \varepsilon_p \left[\int \chi_{0p_z} z \, d\vec{r} \right]^2$$

As we can see this sum cannot be reduced to a product of single

sums. The overlap energy terms involving s- and p- states are easily incorporated with the short range potential terms. The familiar ion-size terms are obtained when factorizing similar pseudopotential terms. The total ion-size correction for a Hamiltonian matrix element is:

$$\frac{1}{4} F_{i0}(0,R_i) F_{j0}(0,R_j)\, A$$
$$+ \frac{1}{8} F_{i0}(0,R_i) F_{j0}^{(2)}(0,R_j) + F_{i0}^{(2)}(0,R_i) F_{j0}(0,R_j)\, J'$$
$$+ \frac{9}{4} F_{i1}^{(1)}(0,R_i) F_{j1}^{(1)}(0,R_j)\, \hat{R}_i \cdot \hat{R}_j\, J$$

The treatment of outer shells is hardly different from the defect problem. The matrix element for the short range potential is:

$$\sum_{\vec{l}} \sum_{\vec{l}'} e^{-i\vec{K}(\vec{l}-\vec{l}')} \langle G_i(\vec{r}-\vec{R}_i) | V^{OUTER}(r) | G_j(\vec{r}-\vec{R}_j) \rangle$$

The interpolation formulas for V_{sk} and V_{sc} are used in this irreducible double sum. The computing time required for the execution of these double sums can be drastically reduced if the gaussians are symmetrically placed in the unit cell, providing that $\vec{k}$ is a special symmetry vector of the Brillouin zone.

The overlap energy terms is easily calculated once the outer shell overlaps are evaluated for the overlap matrix:

$$\sum \varepsilon_\lambda \langle \Phi_i | X_\lambda \rangle \langle X_\lambda | \Phi_j \rangle =$$
$$\varepsilon_s \left(\sum_{\vec{h}} e^{-i\vec{K}\vec{h}} SSOV_i(R_i) \right) \left(\sum_{\vec{h}'} e^{i\vec{K}\vec{h}'} SSOV_j(R_j) \right)$$
$$+ \varepsilon_p \left(\sum_{\vec{h}} e^{-i\vec{K}\vec{h}} SP\sigma OV_i(R_i) \frac{R_{ix}}{R_i} \right) \left(\sum_{\vec{h}'} e^{i\vec{K}\vec{h}'} SP\sigma OV_j(R_j) \frac{R_{jx}}{R_j} \right)$$
$$+ \varepsilon_p \left(\sum_{\vec{h}} e^{-i\vec{K}\vec{h}} SP\sigma OV_i(R_i) \frac{R_{iy}}{R_i} \right) \left(\sum_{\vec{h}'} e^{i\vec{K}\vec{h}'} SP\sigma OV_j(R_j) \frac{R_{jy}}{R_j} \right)$$

$$+ \sum_p \left(\sum_{\vec{n}} e^{-i\vec{k}\vec{n}} S P \sigma O V_i(R_i) \frac{R_{i2}}{R_i} \right) \left(\sum_{\vec{n}} e^{i\vec{k}\vec{n}'} S P \sigma O V_j(R_j) \frac{R_{j2}}{R_j} \right) \quad (104)$$

Section II Conduction State Energy

The above hybrid pseudopotential procedure allows the energy calculation of the excited electron of any $\vec{k}$. We are interested in the lowest posible energy of the excited state, a Γ_1 state ($\vec{k} = 0$). This greatly simplifies the expresions in that all the phase factors are equal to one. The next step in the problem is choosing and placing the floating gaussians in the unit cell. In our preliminary work, we used only one basis centered on an interstice, at the border of a cell. The damping parameter is varied until a minimum in energy is reached. This single gaussian calculation can give a good estimate of the damping parameters that should be used in the many gaussian bases calculation, and it also give a first estimate of the Γ_1 energy. It is worth noting that no minimum is attained when the single gaussian is placed on an atom instead of the interstice. It was observed though, that the tendency was to make the gaussian as flat as possible. Indeed, the maximum electron density isn't located on the atomic sites themselves but mostly in the interstice, between the atoms.

To obtain a more accurate energy, we used a set of 19 bases of the same parameter value as that in the corresponding single gaussian calculation for the rare gas in question. One

Table XVI

	T = 0K	T = tr. pt
Ne	0.1036 (.120) 0.0888 0.0836	0.0982 (.115) 0.0845 0.0800
Ar	0.0691 (.095)	0.0620 (.090)
Kr	0.0783 (.095)	0.0690 (.085)

Γ_1 energies for Ne, Ar and Kr. The first column gives the energies when the lattice parameter at T = 0K of each solid is used. The second column is the same except the lattice spacing at the triple point temperature is used. Refer to Table XIV for triple point temperatures and lattice spacings. The first row for each element is the single gaussian energy with the value of the optimum gaussian parameter appearing in parenthesis. For Ne, two additional calculations are presented. The second row employs two optimized bases: one on the interstice (α = .060) and one on the atom (α = .120). The third row is the 19 bases calculation also used to determine the energies of higher states. Actually, for the state the gaussians are grouped into three symmetrized bases. Practically, it is a three-bases calculation. In atomic units.

basis is placed at the center, six along the cubic axes and 12 on the face diagonal axes. With these bases, not only the Γ_1 symmetry states are obtained but also the p-like Γ_{15} symmetry and the d-like Γ_{12} and Γ_{25}' symmetries. This demonstrates in a particularly striking way the versatility of the floating basis approach. These states are of no concern in the bubble stability problem, but are interesting enough to compare with band calculations of other authors (a paper on our band calculation for Ne and Ar is to be published).

For Ar and Kr, multibases calculations gives energies that are too low for Γ_1. However the relative distances between higher conduction states are in good agreement. The prob-

lem can be traced to inadequacies of the fit of the individual pseudopotential terms for the Ar and Kr atoms in the compact gaussian region (i.e. $\alpha > .08$ a) (see Table V for RMS deviations). For instance, the attractive terms involve a large number of integrals because of the double summation. Any systematic underestimation or overestimation in the evaluation of all these integrals will surely show its effects in the total. The same applies for the overlap integrals sums. Systematic deviations do occur in all fits. In Ne (see Tables II, III and IV), it is observable to a smaller extent. This sort of thing is inherent to our interpolation scheme. The best way of dealing with this is to improve the individual fit when needed. This can be done by using a larger number of gaussians to represent the various pseudopotential terms. Time wasn't available to determine the most efficient way of refitting the terms. The single optimized gaussian energies will therefore be the ones that will be compared to the electron bubble energies, since they have been determined for all three solids. Multibases calculation of Γ_1 for Ne are also reported because they are considered more accurate in the case of Neon.

Below are breifly described the methods used by the several authors which have published band structure calculations.[22-34, 41] Only values which are readily comparable to ours are listed in Table XVII. Values that are not shown are the ones which are calculated with a method that employs a statistical exchange instead of the non-local HF exchange. The statistical exchange probably includes some correlation effects, but these can certainly be taken into account as a pertubation once the band structure is

Table XVII

	Ne	Ar	Kr
Present work	0.104 0.089 0.084	0.069	0.078
KKR (ref. 41)	0.092		
OPW (refs 22 and 24)		0.083	0.081
Mixed Basis (ref. 26)		0.089	
OPW with GTO (refs 33 and 34)	0.073	0.118	
APW (ref. 25)	0.098	0.122	
APW (refs 30 and 31)	0.092	0.096	
LCLFB (refs 27 and 28)	0.081	0.103	0.098
LCLFB with GTO (ref. 29)	0.105		

Hartree-fock conduction band energy (Hr) for Γ_1 in Neon, Argon and Krypton. No polarization or correlation are included in these values. The three values presented for Ne ot the top of the table are the same that appear in Table XVI.

known (see ref. 27). In one of the works that did not have the HF exchange (ref. 23), the KKR method is used. The constant potential outside the muffin-tin sphere was adjusted to give the correct gap energy, thus making it impossible to determine absolute energies (i.e. energy with respect to the vacuum). Reference 41 also presents a KKR calculation on Ne, but here, the absolute energies of the conduction band states are given. The authors used a theoretical calculation of the isolated Neon atom phase shifts in the HF approximation. Lipari[22] and Lipari and Fowler[24] used the OPW method with free-atom wavefunctions and eigenvalues for the core state. In ref. 26 Lipari reported results of a mixed

basis calculation in Ar. Mixed basis means that both the Slater tvpe valence orbitals and the plane waves are determined self-consistentlv. Dagens and Perrot used a modified APW method for Ne and Ar. The same thing was done in refs 30 and 31 except that the required logarithmic derivatives are obtained from static-exchange electron-atom scattering phase shifts. The authors of ref. 41 used the same theoretical phase shifts. Not surprisinglv, ref. 41 and ref. 31 report almost identical results for the conduction states of points Γ, X and L. References 26 and 27 combine to give results for Ne, Ar and Kr using the linear combination of local basis functions with Slater tvpe functions. Here, the term local functions refer to functions centered onlv on the atomic sites. The author of ref. 29 did essentiallv the same thing except that he used gaussians instead of exponentials. The values from ref. 32 are not included in the table because the correlation is alreadv incorporated in the different local tvpe exchange terms they compared. References 32 and 33 presents results for Ne and Ar, respectivelv. The authors use the OPW method with gaussian tvpe orbitals for the core states. Onlv in the Ar case, the outer orbitals are determined self-consistentlv, similarlv to the mixed basis method where the orbitals are of Slater tvpe. In the above there are methods which have a self-consistent character and some which don't. The ones that have are the mixed basis method of ref. 26, the LCLBF method of refs 27 and 28, the local gaussian method of ref. 29 and the OPW method of ref. 34 (for Ar).

Section III Correlation and Polarization

In the above, the calculations do not include correlation between the extra electron and the other electrons. In the one-electron HF theory particles (electron or holes) are treated as being influenced only by the average field produced by the nuclei and other electrons. In general, this approximation is not correct, for one expects that the excess charge, especially if it is moving slowly compared to the other bound electrons, will polarize the surrounding atoms to some degree. The two methods which were used in previous works are based on a classical approach and a quantum mechanical one.

III.a) Classical Formulation

The classical problem as formulated by Fowler[35] is this: Given an extra point charge located on a particular site, calculate the induced dipole moment on each atom due to both the extra electron and the induced moments on the other atoms. This can be done easily using the Mott-Littleton scheme.[14] The value obtained for polarization energy in this static approximation should serve as the upper limit to the true value, since allowing the particle to move will decrease the magnitude of the polarization. In the extreme case where the extra electron moves very rapidly, the electrons of the crystal would perceive this electron as a 'blur' that covers the whole solid. This charge distribution produces no electric field on the atoms, and no polarization will result.

The polarization energy for the electron in some insulators has been calculated by Fowler using the 0th order Mott-Littleton approximation. It was assumed that the point charge is

located at the center af a cell and polarizes the surrounding. Dagens and Perrot[25] pointed out that Fowler did not include the electronic correlation between the electron and the electrons of the same unit cell. This is due to the fact that the Mott-Littleton is a strictly classical theory. Since the electron is centered on an atom there is no electric field at that site, and there is no way to include a classical contribution for that atom. From experimental optical band gap data, Dagens and Perrot estimated 'in reverse' how big this contribution should be. For the Ne case they found a value of -.0386 Hr, and for Ar, it is -.0676 Hr. They also calculated these values another way with the help of a crude scaling law and the first principles calculation of the polarization potential for the ions Na+ and K+ (they are isoelectronic with Ne and Ar) performed by Callaway (a reference is given in their paper). They get -.0401 Hr and -.0643 Hr for Ne and Ar, respectively, which is a quite good agreement.

In our own calculation we use a method which not only takes into account the contribution of all atoms but also is completely classical. It is really the same one as Fowler's except that the charge is centered on an interstice instead of an atom. The main advantage here is that we don't have to rely on estimates of the type D.-P. made for the central atom. Another modification is that we substituted the point charge by a gaussian charge distribution. Making this last change is equivalent to allowing the charge to move in the lattice. The next step is to choose the gaussian's damping parameter. There is very little that guides us in determining the suitable damping factor. Lacking any alternatives,

the gaussian which minimizes the Γ_1 energy in a single gaussian variational calculation is used. Also the effect of orthogonalizing the gaussian is neglected. Table XVIII lists the polarization energy correction according to this method for the extended state in the rare gas solids.

Table XVIII

	Ne		Ar		Kr	
	T=0K	T=24K	T=0K	T=83K	T=0K	T=115k
gaussian damping factor	.120	.115	.095	.090	.095	.085
E_{pol}	.037	.035	.066	.060	.075	.067
$E_{pol}^{ref\ 35}$	.025		.040		.040	
$E_{pol}^{ref\ 28}$	.068		.062		.051	

Values of polarization energy corrections for the Γ_1 conduction state. The correction changes for different tempreratures by virtue of the expansion of the lattice. The correletion energy from ref. 35 is Fowler's, and the one from ref. 28 is Kunz's. All in atomic units.

III.b) Quantum Mechanical Approach

In more recent work, simple pertubation theory is employed to calculate the correlation energy associated with a lone electron in the conduction band. Kunz[29,37] defined approximate expressions for correlation which are evaluated using the electron polaron technique of Toyozawa by 2nd order pertubation. Kunz[37] and Inoue et al.[36] arrive at the same final expression for the correlation energy:

$$\Delta E^{(2)}(\vec{k}) = -\sum_{g} \frac{|V_g(o)|^2}{E(k-g)-\varepsilon-E(k)} \qquad (105)$$

where

$$V_q(0) = e\left(\frac{2\pi\mathcal{E}(1-1/K_0)}{V}\right)^{1/2} \frac{i}{q} \int \phi(\vec{r}) e^{i\vec{q}\cdot\vec{r}} \phi(r) d\vec{r}$$

$E(\vec{k})$ are the HF band energies, $\sum(\vec{q})$ is the summation over the 1st brillouin zone, $\mathcal{E}$ is the exciton energy assumed constant for all $\vec{q}$, $\phi(\vec{r})$ is the localized function which forms the Bloch function of the electron in question and K_0 is the dielectric constant. In $\sum(\vec{q})$ the summation extends, in principle, to higher conduction level but we shall neglect them since they are expected to give a small contribution. Only levels that are close in energies to the $E(\vec{k})$ are needed in the summation. The expression is simplified if gaussians are used and

$$\Delta E^{(2)}(k) = \frac{e^2}{4\pi^2}\left(1-\frac{1}{K_0}\right)\int d\vec{q}\, \frac{1}{q^2} \exp\left(\frac{-q^2}{8\alpha}\right) \frac{\mathcal{E}}{E(k)+\mathcal{E}-E(k-q)} \qquad (106)$$

where

$$N_\alpha^2 \int e^{-2\alpha r^2} e^{-i\vec{q}\cdot\vec{r}} d\vec{r} = \exp\left\{\frac{-q^2}{8\alpha}\right\}$$

To evaluate this we must know $E(\vec{k})$ for the whole Brillouin zone. As an approximation, we can put $E(\vec{k})$ as being constant for all $\vec{k}$, and convert the brillouin zone integral to a sphere of equal volume. To simplify further we put $\mathcal{E}$ greater than the bandwidth such that the rightmost factor in the integral becomes practically unity. We have done this only to obtain a ball-park figure for the correlation.

$$\Delta E^{(2)}(k=0) = \frac{e^2}{4\pi^2}\left(1-\frac{1}{K_0}\right)\int d\vec{q}\, \frac{1}{q^2} \exp\left(\frac{-q^2}{8\alpha}\right)$$

$$= \frac{e^2}{4\pi^2}\left(1-\frac{1}{K_0}\right) 4\pi \int_0^R dq \exp\left(\frac{-q^2}{8\alpha}\right) \quad ; \quad R = \left(\frac{24\pi^2}{a^3}\right)^{1/3}$$

$$\Delta E^{(2)}(k=0) = e^2\left(1-\frac{1}{K_0}\right)\left(\frac{2\alpha}{\pi}\right)^{1/2} erf\left(\frac{(3\pi^2)^{1/3}}{a(2\alpha)^{1/2}}\right) \qquad (107)$$

For Ne, a typical case, α_s = .12 a_o, a = 8.435 a_o, K_o = 1.2387, and the correlation correction is .0378 Hr. This agrees with the value of .037 Hr obtained using our classical model. Of course, it is coincidental that both values are very close. Because we are not in a postion of making precise calculations of the integral in $\vec{q}$ we decided to use the Fowler method.

Table XIX

	T = 0K	T = tr.pt
Ne	0.067 0.058 0.054 0.047	0.063 0.053 0.059 0.045
Ar	0.003 0.040	0.002 0.035
Kr	0.003 0.033	0.002 0.032

Γ_1 energies with correlation of the present work compared to the electron bubble energy. The first column for each temperature is the conduction state energy, and the second one is the electron bubble energy. The three values for the conduction state in Ne are explained in Table XVI. In atomic units.

Section IV Stability of electron states

Table XIX presents the final results of the thesis. Considering only the conduction state calculation which used an optimized gaussian, one would conclude that the electron bubble is stable in solid Ne. This isn't true experimentally. In the introduction, it was mentioned that electron bubble occured in Neon only in the liquid form. This obviously suggest to us that the single optimized gaussian calculation of the lowest conduction

Table XX

	Ne	Ar	Kr
present work	0.067 0.054 0.047	0.003	0.003
ref. 28	0.013	0.041	0.047
ref. 41	0.047		
ref. 24		0.003	

Γ_1 energies with correlation reported by some authors. Reference 28 uses the electron polaron technique for the pertubative correction for correlation effects (see text). Reference 41 uses experimental phase shifts to calculate new conduction states. The many-body effects are thus implicitly taken into account. Fowler's method is used in ref. 24.

state is not good enough. The two other calculations (which uses a larger number of gaussian bases), however, give sufficiently low energies for the agreement. An interesting thing to observe is that going from the absolute zero to the triple point temperature, the difference in energy of the localized state and the extended state decreases. This makes the electron bubble stable in solids of sufficiently low density. These low density solids don't occur since they expand too little before they melt. If a rare gas liquid can be roughly regarded as a solid of lower density than usual, then our theory suggests that the electron bubble could be stable in liquid Neon. This can be tested by simulating a liquid by a solid of lattice parameter that would give the solid the same density as that of the liquid. Some attempts have been made to calculate the electron bubble and the 'conduction state' energies in this solid of liquid density. The major obstacle encountered

is the very large lattice deformation around the excess electron. Here, not only our lattice free energy treatment becomes difficult, but also the thirteen shell displacements do not converge as fast as in the normal solid case. More movable shells are needed. The above only shows that the treatment of liquids is more complex than that of solids. As far as the other two rare gases are concerned, it is clear that even if the band calculation isn't up to par, the difference in energies between the two types of states is so large that there is little doubt that the conduction state is the stable state.

Glancing at Table XX, we see a wide dispersion of conduction state energy. It is odd to see that in ref. 28 the conduction state energy with correlation is lower in Neon than in Argon and Krypton. This goes against out initial beliefs. One would think that the ordering would be reversed in view of the experimental electron affinity data (ref. 6). Moreover, using their Γ_1 energies for Ne and Ar, we would obtain an electron bubble marginally stable in the Ar solid while it would be definitely nonexistant in solid Ne! As for the ordering of conduction state energies without correlation of the present work, it shouldn't be surprising that the Γ_1 energy of Kr turned out higher than the Ar's since the pseudopotential terms for Kr were difficult to fit for gaussian factor above .08. The ordering of the Γ_1 energies with correlation for the rare gas solids is what was expected. That is, at least the Ar conduction band minimum doesn't lie lower than Kr's (they are the same).

Chapter IV

Conclusion

The aim of this work was to determine the stability of the electron bubble in rare gas solids with respect to the lowest energy conduction state. A hybrid pseudopotential was used to treat both types of excited electron states. Our results agreed with experimental evidence that excess electrons occupy extended states. The difference in energy of the two states in RGS increases slightly as the temperature approaches zero. This density related tendency suggests the possibility of stable electron bubble in the rare gas liquids, most probably in Neon since the electron bubble in solid Neon is marginally unstable.

In the band calculation part of this work we introduced an application of off-center gaussian functions. In earlier papers on band calculations the functions, of exponential or gaussian type, were invariably placed on atomic sites. It is a well known fact that electrons in a conduction state spend most of its time between atoms rather than on them. This is why a gaussian was placed on the interstice in our single optimized gaussian calculation of Γ_1. Perhaps it is impractical to do so in a self-consistent HF band calculation because it would entail a slow convergence for the valence bands. The valence orbitals are indeed very well described by functions centered on nuclei. On the other hand, a pseudopotential calculation does not compute valence orbitals. Therefore these off-center bases seems to be the ideal type to use here.

The work also showed that the slow-varying approximation

for the pseudowavefunction, an idea initiated by BSG, can only be applied to compact core orbitals. The other larger orbitals are treated exactly with the use of interpolation formulae. These formulae can be as accurate as one would like; it is only a question of how many more parameters one wants to introduce. For Ar and especially Kr, better interpolation formulae are required to obtain better conduction band energies. Some attention is presently being given to this subject. Other than that, the hybrid method is very efficient to apply.

Some important comments should be restated concerning the electron bubble calculation. It was shown in the interatomic potential section of chapter II that the relatively large compression between atoms close to the defect makes the deformation energy value uncertain, as no interatomic potential is accurate for large compressions. In a potential derived from the properties of the solid only the neighbourhood of its minimum is the reliable part. Since nothing short of a self-consistent HF cluster calculation is available to determine accurately the shape of the potential curve for large compressions, we were obliged to use interatomic potentials from gas data. An approximation that can be questioned is the point dipole approximation of the atoms in the presence of a net charge. This approximation is widely used, but only in cases where atomic displacements are small or zero. In the bubble case compressions of about 15% is expected to modify the electronic wavefunctions and the atomic polarizability. The extent of the changes are unknown and can't be evaluated easily. The atomic polarizability are simply left constant throughout the lattice relaxation process. Improvement on the two topics above

is really a matter of obtaining better data or additional data that are not available. The last remark on the bubble calculation is about the formalism developped to treat the lattice free energy for the Ne solid. It was only intended as an approximation of the effects of displaced atoms on the free energy. It turns out that there are problems related to the large displacements. As it is, the scheme cannot be improved further. The next best method is to calculate the deformed lattice's new normal mode frequencies, but this is much more complicated. One could possibly try to combine these two schemes so that each would be applied to the atoms with which the application is easiest. Our own method would calculate the change in free energy for the toms of shells further than the 3rd, as we have it already and the normal mode calculation would apply to the first three shell atoms.

Related work on the self-trapped exciton (STE) and the rare gas impurity states in Neon is worth mentioning here. These calculations are very similar to the one on electron bubble. The only difference is the presence of an atom at the vacancy site. The theoretical values which can be readily tested by experiment are the transition energies. The calculated absorption energy of the STE for Γ_1 to Γ_{15} (atomic 3s to 3p) is 2.13 eV while the experimental value is 2.13 eV, which is a good agreement. The bubble of the exciton is just a little smaller than that of the excess electron (d_1 = 2.31 a_0 for electron and d_1 = 2.24 a_0 for exciton). This is because the attraction between the hole and the electron renders the electron wavefunction more compact, thus exerting less force on the surrounding atoms. For the impurity states, we want to compare experimental and theoretical transition

energies for the absorption and emission. The ground state of the system is the np hole state. Here, it is not necessary to know the absolute hole state energy because it is assumed unaffected by the atoms nearby. This is not really true since there is slight overlap between the impurity np state and the nearby Ne atoms, making the hole state energy higher than estimated. Our pseudopotential theory cannot treat hole states anyways. The next state is the (n+1)s impurity state. This state is calculated using our hybrid pseudopotential method. The time for the absorption and emission transition is very short such that the lattice can be considered rigid during the process. Because an impurity atom and the host matrix atoms are of different size there is some deformation of the lattice in the neighbourhood of the defect. All the atom, though, are in close contact with each other. Once the absorption is complete, the lattice begins to relax to form a bubble around the defect, and the energy of the (n+1)s state is lowered. After equilibrium is reached (after a few atomic vibrations) the impurity emits a photon. Since the transition occurs with a different lattice configuration the transition energy is expected to be different. The difference is called the Stokes' shift. The calculated Stokes' shift for Ar, Kr and Xe impurites in solid Ne are 1.21, 1.21 and 1.33 eV, respectively. The experimental values are .81, .50 and .45 eV in the same order. For comparison's sake the same thing can be done for the Neon atom in Neon solid; the Ne atom is treated as an impurity. The calculated and experimental Stokes' shifts are .99 and .72, respectively. The overall agreement is satisfactory in view of the approximations that were made. For instance, the hole

state energy is supposed to be higher for the slightly deformed lattice than for the lattice when the bubble is formed. This is because the hole state has practically zero overlap with the atoms that have been greatly displaced while in the other case the overlap is small but probably non-negligable. Underestimating the energy of the intial state of the absportion transition will make the calculated Stokes' shift deviate the way it does. Work on the alkali atom impurity is presently in progress.

Appendix A

Calculation of Coulomb Integral

In general this is a three center integral. The following expression is the contribution of one atom to the short range Coulomb matrix element between two gaussians at position R_i and R_j.

$$\langle \phi_i | V_{sc,\gamma} | \phi_j \rangle = N_j N_i \int e^{-\alpha_i r_i^2} V_{sc,\gamma}\, e^{-\alpha_j r_j^2} d\vec{r} \qquad (A1)$$

$$V_{sc,\gamma} = \frac{-Z_\gamma}{|\vec{r} - \vec{R}_\gamma|} + 2\sum_\lambda \int \frac{|\chi_{c\lambda}(\vec{r}' - \vec{R}_\gamma)|^2}{|\vec{r} - \vec{r}'|} d\vec{r}' \qquad (A2)$$

where $\vec{r}_i = \vec{r} - \vec{R}_i$ and $\vec{r}_j = \vec{r} - \vec{R}_j$

In the hybrid scheme we treat only the outer electrons exactly. For neutral rare gas atoms, the above integral involve eight electrons. To keep the integral in $\vec{r}$ from diverging we take the nuclear charge in $V_{sc}(\vec{r})$ as being +8. The rest of the nuclear charge is included in the calculation of the ion-size parameters, A, J' and J. Since $V_{sc}(\vec{r})$ is a fuction of radial symmetry about $\vec{R}_\gamma$, we take $\vec{R}_\gamma$ as a new origin and $\vec{r}$ as the position vector relative to the new origin. This integral is determined analytically for values of r ranging from 0 to 20 a_o with an interval of .08 a_o. The gaussian factors in the integrand are not radial functions of r. Their spherically symmetric component is extracted as follows: The two gaussians can be expressed as a single gaussian easily:

$$e^{-\alpha_i r_i^2} e^{-\alpha_j r_j^2} = \exp\left(-\frac{\alpha_i \alpha_j}{\alpha_i + \alpha_j} |\vec{R}_i - \vec{R}_j|^2\right) e^{-(\alpha_j + \alpha_i) r_k^2}$$

$$\text{where} \quad \vec{r}_k = \vec{r} - \vec{R}_k \quad \text{and} \quad \vec{R}_k = \frac{(\alpha_i \vec{R}_i + \alpha_j \vec{R}_j)}{\alpha_i + \alpha_j} \qquad (A3)$$

The next step is to expand this gaussian in a Fourier-Legendre series and to conserve the first term (the other higher order terms integrate to zero by symmetry).

$$e^{-\alpha r_k^2} = \sum_\ell \frac{(2\ell+1)}{2} F_\ell(r, R_k)\, P_\ell(\cos\theta_k) \qquad (A4)$$

where $F_\ell(r, R_k) = \int_{-1}^{1} e^{-\alpha r_k^2} P_\ell(\cos\theta_k)\, d(\cos\theta_k)$ and $\cos\theta_k = \hat{r} \cdot \hat{R}_k$.

The first term is:

$$\frac{1}{2} F_0(r, R_k) = \frac{1}{2} \int_{-1}^{1} e^{-\alpha(r^2 + R_k^2 - 2rR_k\cos\theta_k)}\, d(\cos\theta_k)$$

$$= \frac{1}{2} \frac{e^{-\alpha(r^2+R_k^2)}}{2rR_k\alpha} \left[e^{2rR_k x} \right]_{x=-1}^{x=1}$$

$$= \frac{e^{-\alpha(r^2+R_k^2)}}{2rR_k\alpha} \sinh(2\alpha r R_k) \qquad (A5)$$

When $r=0$ (i.e. when the gaussian is centered on the atom), $(1/2)F_0(r, R_k)$ reduces to $e^{-\alpha R_k^2}$, as expected. Both factors in the r integral being radial functions, the integration is written:

$$4\pi N_i N_j \exp\left(-\frac{\alpha_i\alpha_j}{\alpha_i+\alpha_j}|\vec{R}_i - \vec{R}_j|^2\right) \frac{e^{-\alpha R_k^2}}{2\alpha R_k} \int e^{-\alpha r^2} \sinh(2\alpha r R_k)\, V_{sc}(r)\, r\, dr \qquad (A6)$$

which can be calculated numerically by the Simpson's method.

If the χ's were expressed in gaussians instead of Slater type functions, the computation of the double integral can be performed analytically using the formulae given by Shavitt in reference 40.

Appendix B

Calculation of Exchange Energy

This integral is special in that it is a two-electron integral; the gaussian factrs are functions integrated in different coordinates. The contribution of an atom at site $\vec{R}_\gamma$ to the matrix element between a gaussian on $\vec{R}_i$ and another on $\vec{R}_j$ is

$$N_i N_j \sum_\lambda \int e^{-\alpha_i(\vec{r}_1-\vec{R}_i)^2}\, \chi_{o\lambda}(\vec{r}_1-\vec{R}_{i\gamma}) \left[\int \frac{\chi_{o\lambda}(\vec{r}_2-\vec{R}_{j\gamma}) e^{-\alpha_j(\vec{r}_2-\vec{R}_j)^2}}{|\vec{r}_1-\vec{r}_2|} d\vec{r}_2\right] d\vec{r}_1 \qquad (B1)$$

where the subscript i refers to the gaussian on $\vec{R}_i$ and the subscript j refers to the gaussian on $\vec{R}_j$. Because the χ's are expressed in Slater type functions, the integrals are just about hopeless to calculate exactly. However, converting the Slater radial functions to a set of gaussian functions allows an analytical evaluation of the integrals. In our hybrid scheme, we have only one s-type and one p-type orbital to fit. We will examine a particular case in detail. Take the Ne 2s radial function:

$$R_s(r) = \sum_i c_i N_i r^{n_i} e^{-\alpha_i r} \quad ; \quad N_i = \frac{(2\alpha)^{n_i+3/2}}{[(2n+2)!]^{1/2}} \qquad (B2)$$

where

i	c_i	n_i	α_i
1	-0.23093	0	9.48486
2	-0.00635	0	15.56590
3	0.18620	1	1.96184
4	0.66899	1	2.86423
5	0.30910	1	4.32530
6	-0.13871	1	7.79242

The Ne 2p orbital is similar where we have

$$R_p(r) = \sum_i c_i N_i r^{n_i} e^{-\alpha_i r} \qquad (B3)$$

Here the c_i's, the n_i's, the α_i's and even the number of bases may be different. Note that the lowest possible power of the factor r in the s orbital is 0 while for the p orbital it is 1. The

gaussian tvpe orbital we want for the Ne 2s is written

$$R_s^{GAUSS.}(r) = \sum_i^N c_i e^{-\alpha_i r^2} \qquad (B4)$$

where c_i and α_i are the adjustable parameters. As was suggested bv R. Stewart,[39] only ls tvpe gaussians are used in this expansion. Functions such as $r\exp(-\alpha r^2)$, $r^2\exp(-\alpha r^2)$ and so on are not needed to obtain good accuracv. There are two ways to proceed from here. One is to use a small number of bases (sav, the same number as in the original Slater function, 6). Both set of parameters c_i and α_i are to be optimized. The c_i's can be easilv determined bv least squares method and the α_i's must be found bv the direct method of variation to search for a local minimum. The alternative is to enlarge the number of bases, sav N=15, and to use the same bases gaussians for all applications. The gaussian's dampin parameter remain fixed at

$$\alpha_i = .1 \cdot 2^{(i-1)}$$

The large number of bases makes up for the fact that the 's are not optimized. The same procedure is used for the outer p radial function except that:

$$R_p^{GAUSS}(r) = \sum_i c_i r e^{-\alpha_i r^2} \qquad (B5)$$

The α_i's are the same as before.

The contributions of the two types of orbitals are calculated separatelv. For the s orbital, we have:

$$N_i N_j \sum_{m,n} c_m c_n \int e^{-\alpha_i (\vec{r}_1 - \vec{R}_i)^2} e^{-\alpha_m r_1^2} \left[\int \frac{e^{-\alpha_n r_2^2} e^{-\alpha_j (\vec{r}_2 - \vec{R}_j)^2} d\vec{r}_2}{|\vec{r}_1 - \vec{r}_2|} \right] d\vec{r}_1 \qquad (B6)$$

Each term of the double sum is

$$C \exp(-\mathcal{U} R_i^2 - \mathcal{V} R_j^2) F_0[\omega \overline{PQ}^2]$$

where

$$C = \frac{2\pi^{5/2}}{(\alpha_i+\alpha_m)(\alpha_j+\alpha_n)(\alpha_i+\alpha_j+\alpha_n+\alpha_m)^{1/2}} ,$$

$$U = \frac{\alpha_i \alpha_m}{(\alpha_i+\alpha_m)} , \quad V = \frac{\alpha_j \alpha_n}{(\alpha_j+\alpha_n)} ,$$

$$W = \frac{(\alpha_i+\alpha_m)(\alpha_j+\alpha_n)}{(\alpha_i+\alpha_j+\alpha_m+\alpha_n)} , \quad F_0(t) = \frac{1}{2}\left(\frac{\pi}{t}\right)^{1/2} \mathrm{erf}(\sqrt{t})$$

and $$\overline{PQ}^2 = \left| \frac{\alpha_i \vec{R}_i}{(\alpha_i+\alpha_m)} - \frac{\alpha_j \vec{R}_j}{(\alpha_j+\alpha_n)} \right|^2$$

This is a special case of the four-center integral with two gaussians centered at the origin. The more general expression is a little more complicated and can be found in ref. 46. The reference also gives the method to determine the p orbital contribution. The method relies on the fact that a p orbital centered on $\vec{R}_0$ can be written:

$$(z-Z_0)e^{-\alpha(\vec{r}-\vec{R}_0)^2} = \frac{1}{2\alpha}\frac{\partial}{\partial Z_0} e^{-\alpha(\vec{r}-\vec{R}_0)^2} \qquad (B7)$$

The p_z orbital contribution is then obtained by differentiating the general expression twice with respect to the Z_0 coordinate of the gaussians n and m (they are centered on the same site, the origin), and by dividing the result by $4\alpha_n\alpha_m$. Of course, this does not work on equation (B6) since it is a special case of a general expression. The double differentiation results in a complicated expression which simplifies a little when R_0 is put equal to zero. The orbitals p_x and p_y are treated identically, and the sum is:

$$C\exp(-UR_i^2 - VR_j^2)\frac{1}{4\alpha_n\alpha_m}\left\{ -F_2[W\overline{PQ}^2]\, 4\alpha_m\alpha_n \frac{W^2\overline{PQ}^2}{(\alpha_i+\alpha_m)(\alpha_j+\alpha_n)} \right.$$

$$\left. + F_1[W\overline{PQ}^2]\, 4W\left(\frac{U\alpha_n}{(\alpha_j+\alpha_n)}\vec{PQ}\cdot\vec{R}_i + V\frac{\alpha_m}{\alpha_i+\alpha_m}\vec{PQ}\cdot(-R_j)\right)\right.$$

$$+6F_1[\omega\overline{PQ}^2]\frac{\omega\alpha_m\alpha_n}{(\alpha_i+\alpha_m)(\alpha_j+\alpha_n)} + F_0[\omega\overline{PQ}^2]4uv\vec{R}_i\cdot\vec{R}_j\Big\}$$

where $F_{n+1}(t) = -\frac{d}{dt}F_n(t)$, that is

$$F_1(t) = \frac{1}{2t}[F_0(t) - e^{-t}]$$

and $$F_2(t) = \frac{1}{2t}[3F_1(t) - e^{-t}].$$

Appendix C

Typical Matrix Element in SVA

We wish to derive the off-diagonal element for the overlap according to the slow varying approximation of the pseudowavefunction. We write the overlap contribution of a core:

$$\sum_{\lambda} \langle \phi_i(|\vec{r}-\vec{R}_i|) | \chi_\lambda(r) \rangle \langle \chi_\lambda(r) | \phi_j(|\vec{r}-\vec{R}_j|) \rangle$$

$\vec{R}_i$ and $\vec{R}_j$ are the positions relative to the core site of the pseudofunctions i and j. One of the factors are expanded up to the first order terms:

$$\langle \phi_i(|\vec{r}-\vec{R}_i|) | \chi_\lambda(r) \rangle = 2\pi \langle F_{io}(o,R_i)\, Y_{oo}(\hat{r}) Y_{oo}^*(\hat{R}_i) + F_{io}^{(2)}(o,R_i) \frac{r^2}{2} Y_{oo}(\hat{r}) Y_{oo}^*(\hat{R}_i)$$
$$+ F_{i1}^{(1)}(o,R_i)\, r \left[Y_{10}(\hat{r}) Y_{10}^*(\hat{R}_i) + Y_{11}(\hat{r}) Y_{11}^*(\hat{R}_i) + Y_{1\bar{1}}(\hat{r}) Y_{1\bar{1}}^*(\hat{R}_j) \right] | \chi_\lambda(r) \rangle \qquad (C.1)$$

For the moment let's restrict ourselves to a single principal quantum number. The sum over λ will consist of one s orbital and three p orbitals. D orbitals do not participate in first order terms. For each λ, different expansion terms vanish from symmetry. When λ = s, the surviving terms are

$$\left\{ 2\pi F_{io}(o,R_i) \langle Y_{oo}(\hat{r}) | \chi_s \rangle Y_{oo}^*(\hat{R}_i) + 2\pi F_{io}^{(2)}(o,R_i) \langle Y_{oo} \frac{r^2}{2} | \chi_s \rangle Y_{oo}^*(R_i) \right\} \times$$
$$\left\{ 2\pi F_{jo}(o,R_j) \langle \chi_s | Y_{oo}(\hat{r}) \rangle Y_{oo}(\hat{R}_j) + 2\pi F_{jo}^{(2)}(o,R_j) \langle \chi_s | Y_{oo} \frac{r^2}{2} \rangle Y_{oo}(R_j) \right\}$$

since $Y_{oo}(\hat{r}) = Y_{oo}(\hat{R}_i) = Y_{oo}(\hat{R}_j) = (4\pi)^{-1/2}$

we get

$$\frac{1}{4} F_{io} F_{jo} \left(\int \chi_s \, d\tau \right)^2 + \frac{1}{8} \left[F_{io} F_{jo}^{(2)} + F_{io}^{(2)} F_{jo} \right] \left(\int \chi_s r^2 \, d\tau \right)^2$$

where the $F_{io}^{(2)} F_{jo}^{(2)}$ is dropped because it becomes a 2nd order term. For a p orbital, say the one with Y_{10} symmetry, only one term sur-

vives:

$$2\pi F_{i1}^{(1)}(0,R_i)\langle Y_{10}(\hat{r})r|\chi_{p0}\rangle Y_{10}^{*}(R_i)\cdot 2\pi F_{j1}^{(1)}(0,R_j)\langle \chi_{p0}|Y_{10}(\hat{r})r\rangle Y_{10}(R_j)$$

substituting

$$Y_{10}(\hat{R}) = \left(\frac{3}{4\pi}\right)^{1/2}\cos\theta$$

we get

$$3\pi F_{i1}^{(1)} F_{j1}^{(1)} Y_{10}^{*}(R_i) Y_{10}(R_j)\left(\int r\cos\theta\,\chi_{p0}\,d\tau\right)^2$$

For the two other p orbitals, similar expressions are obtained, with all the factors bieng the same except the spherical harmonic product. Summing the three expressions, one gets.

$$\frac{9}{4} F_{i1}^{(1)} F_{j1}^{(1)} \left[\hat{R}_i\cdot\hat{R}_j\right]\left(\int r\cos\theta\,\chi_p\,d\tau\right)^2$$

where the spherical harmonic addition theorem was used:

$$\sum_{m=-l}^{l} Y_{lm}^{*}(\hat{r}) Y_{lm}(\hat{r}') = \frac{(2l+1)}{4\pi} P_l(\hat{r}\cdot\hat{r}').$$

The s and p orbitals of different principal quantum number are easilv included since their contributions are simplv summed together. The factorization of these terms results in the ion-size paramters B, K' and K exactlv as defined in equations (27), (28) and (29). The whole procedure can be repeated for the matrix elements of the Coulomd and exchange integrals, giving the parameters A , J' and J .

Appendix D

Slow Varying Approximation Expansion Terms

A gaussian, $\exp(-\alpha|\vec{r}-\vec{R}_o|^2)$ is expanded about an atomic site which we will take as the origin:

$$e^{-\alpha(\vec{r}-\vec{R}_o)^2} = \sum \frac{2l+1}{2} F_l(r, R_o) P_l(\cos\Omega_o) \qquad (D1)$$

$$F_l(r, R_o) = \int_{-1}^{1} e^{-\alpha(\vec{r}-\vec{R}_o)^2} P_l(\cos\Omega_o) d(\cos\Omega_o) \qquad (D2)$$

where Ω_o is the angle between $\vec{r}$ and $\vec{R}_o$. This appendix is concerned with the first few F_l's and their derivatives. $F_o(r,R_o)$ is easy to evaluate:

$$F_o(r, R_o) = \int_{-1}^{1} e^{-\alpha(r^2+R_o^2-2rR_o x)} dx$$

$$= 2\, e^{-\alpha(r^2+R_o^2)} \frac{\sinh(2\alpha r R_o)}{(2\alpha r R_o)} \qquad (D3)$$

and $$F_o(o, R_o) = 2\, e^{-\alpha R_o^2} \qquad (D4)$$

The first derivative of $F_o(r,R_o)$ with respect to r evaluated at r = 0 is zero, which is shown here:

$$F_o^{(1)}(r, R_o) = \frac{d}{dr}\int_{-1}^{1} e^{-\alpha(r^2+R_o^2-2rR_o x)} dx$$

$$= \int_{-1}^{1} \frac{d}{dr} e^{-\alpha(r^2+R_o^2-2rR_o x)} dx \qquad (D5)$$

$$= \int_{-1}^{1} (2\alpha R_o x - 2\alpha r) e^{-\alpha(r^2+R_o^2-2rR_o x)} dx$$

The second term is

$$(-2\alpha r)\left[2\, e^{-\alpha(r^2+R_o^2)} \frac{\sinh(2\alpha r R_o)}{(2\alpha r R_o)}\right]$$

which disappears when r tends to zero. The first term is

$$\frac{2e^{-\alpha(r^2+R_o^2)}}{r}\left(\cosh(2\alpha r R_o) - \frac{\sinh(2\alpha r R_o)}{(2\alpha r R_o)}\right)$$

$$= \int_{-1}^{1} (2\alpha R_0 x^2 - 2\alpha r x) e^{-\alpha(r^2 + R_0^2 - 2rR_0 x)} dx \qquad (D8)$$

We have seen that the second term becomes zero as r = 0, and the first term is the same as the third term of equation (D6) apart from a factor of $2\alpha R_0$. Then,

$$F_1^{(1)}(0, R_0) = \frac{4}{3}\alpha R_0 e^{-\alpha R_0^2} \qquad (D9)$$

As a final note, it must be stated that the simple analytical forms encountered here are attributable to the fact that the gaussian function is a function of distance squared.

Appendix E

Electric Field Due to Atomic Point Dipoles

The field produced by many dipole moments is

$$\vec{E}_{dip}(\vec{r}_n) = \sum_m \frac{3(\vec{\mu}_m \cdot \vec{r}_{mn})\vec{r}_{mn} - r_{mn}^2 \mu_m}{r_{mn}^5} \quad \ldots \quad (E1)$$

where $\vec{r}_{mn} = \vec{r}_m - \vec{r}_n$.

We are in a cubic environment with the electron wavefunction having full cubic symmetry (the electron state is an s-state centered at the origin). If there are any atomic displacements they will be such that they don't destroy the symmetry. Atoms who have the same symmetry coordinates (i.e. atoms of the same shell) share the same magnitude of dipole moment. We will assume that the moment vector of each atom is parallel to the postion vector of the atom. This is equivalent to saying that the electric fields produced by all the other dipoles combine at a lattice site so that the vectorial sum's only component is radial. This is true for atoms of shells consisting of only one symmetry coordinate (e.g. (110), (200), (220), (222), etc...). This is only an approximation for the other atoms. The approximation, which is probably a good one, was adopted because it simplifies the expressions about to be presented. Putting $\vec{E}_{dip} \| \vec{r}$, we have

$$\begin{aligned} |\vec{E}_{dip}(\vec{r}_n)| &= \vec{E}_{dip}(\vec{r}_n) \cdot \hat{r}_n \\ &= \sum_m \frac{3(\vec{\mu}_m \cdot \vec{r}_{mn})(\vec{r}_{mn} \cdot \vec{r}_n) - r_{nm}^2 \vec{\mu}_m \cdot \vec{r}_n}{r_{mn}^5} \\ &= \sum_m \frac{\mu_m 2(r_n^2 + r_m^2)\cos\theta - r_m r_n (3 + \cos^2\theta)}{(r_n^2 + r_m^2 - 2 r_n r_m \cos\theta)^{5/2}} \quad (E2) \end{aligned}$$

with $\cos\theta = \hat{r}_n \cdot \hat{r}_m$

Now we group the unknown μ's into shells:

$$\vec{E}_{dip}(\vec{r}_n) = \sum_{\substack{j \\ \text{shells}}} \mu_j \sum_{\substack{j' \\ \text{atoms in shell } j}} \frac{2(r_n^2 + r_j^2)\cos\theta - r_n r_j (3 + \cos^2\theta)}{(r_n^2 + r_j^2 - 2 r_n r_j \cos\theta)^{5/2}} \qquad (E3)$$

with $\cos\theta = \hat{r}_n \cdot \hat{r}_{jj'}$ and $r_j = |\vec{r}_{jj'}|$

The double sum excludes the case where cos θ = 1 and $\vec{r}_n = \vec{r}_{jj'}$, simultaneously. The lattice is divided into two regions. The inner region, consisting of the first thirteen shells (248 atoms), is alloted the dipole moments which are left unknown. The dipole moments of the outer region (shells farther than the thirteenth) are determined by the continuum model of the dielectric. This gives:

$$E_{dip}(\vec{r}_n) = \sum_{j=1}^{13} \mu_j \sum_{j'}^{no_j} \frac{2(r_n^2 + r_j^2)\cos\theta - r_n r_j (3 + \cos^2\theta)}{(r_n^2 + r_j^2 - 2 r_n r_{jn} \cos\theta)^{5/2}}$$

$$+ \frac{a^3}{16\pi}\left(1 - \frac{1}{k_o}\right) \sum_{j=14}^{\infty} \frac{1}{r_j^2} \sum_{j'}^{no_j} \frac{2(r_n^2 + r_j^2)\cos\theta - r_n r_j (3 + \cos^2\theta)}{(r_n^2 + r_j^2 - 2 r_n r_j \cos\theta)^{5/2}} \qquad (E4)$$

This can be rewritten:

$$\vec{E}_{dip}(\vec{r}_n) = \sum_{j}^{13} \mu_j (SS)_{nj} + (LS)_n \qquad (E5)$$

where the shell summation numbers, $(SS)_{nj}$, are defined

$$(SS)_{nj} = \sum_{j'}^{no_j} \frac{2(r_n^2 + r_j^2)\cos\theta - r_n r_j (3 + \cos^2\theta)}{(r_n^2 + r_j^2 - 2 r_n r_j \cos\theta)^{5/2}}$$

where, again, the summation excludes the term cos θ = 1 if n = j. Note that

$$(SS)_{nj} = (SS)_{jn} \frac{no_j}{no_n} \qquad (E7)$$

because the definition is symmetric in r_j and r_n. The calculations are almost cut by half. $(LS)_i$ stands for lattice sum:

$$(LS)_i = \sum_{j=14} \sum_{j'} \frac{2(r_i^2 + r_j^2)\cos\theta - r_i r_j (3 + \cos^2\theta)}{r_j^2 (r_i^2 + r_j^2 - 2 r_i r_j \cos\theta)^{5/2}} \frac{a^3}{16\pi}\left(1 - \frac{1}{k_o}\right)$$

while the (SS)'s are easy to evaluate, the (LS)'s are a little more difficult owing to the slow convergence of the sum. (LS) of the shells of smaller radius are generally slower to converge to the correct values. If the site where the electric field is to be calculated is close to the origin, there will be large cancellation between electric fields produced by dipoles opposite each other. At the origin, the extreme case, the field is exactly zero. For the first shell, at distance $a/\sqrt{2}$ from the origin, 8000 atoms are needed for the sum to converge to at least 2 correct figures. On the other hand, shells closer to the outside region receive a stronger influence from the exterior shell dipoles. There is hardly any cancellation for the first few shells of the exterior region, since the distances to dipoles of opposite direction are much more disparate. Indeed, to obtain three significant figures for (LS) of the ninth shell through to the thirteenth shell, only 1000 atoms are needed in the summation.

All in all, it is not practical to calculate the (LS)'s in the bubble program since each one of them involve a summation over at least a thousand atoms and they have to be recalculated after each shell displacement. The dipole electric field will therefore include only the inner shell contribution, the $(SS)_{ij}$ terms. This is a reasonable approximation since the dipole moments of the inner region are much greater than those of the outer region. The (LS)'s are expected to bring, at best, a small contribution to the electric field from dipoles. To check this aproximation, one can calculate the (LS)'s once the final configuration of an electron bubble is known, and put them back into equation (E5). The Mott-

Littleton procedure is then carried through. If there is no significant change in polarization energy, then the approximation is good. Alternatively, one suspects that neglecting the outer region dipole moments, will mostly affect the accuracy of the dipole moments calculated for the inner shells lying closer to the outer region. This is demonstrated in Tables XI and XIV of the second chapter. Using the continuum model values for these shells should give a difference in polarization energy that is typical of the precision of the approximation. For the Ne electron bubble at T = 0K, the difference is very small: 2 x 10-5 Hr. For Xr , which is much more polarizable, it is 3 x 10-4 Hr, fifteen times greater than in Ne but is, nonetheless, less than 1% of the polarization energy of 4.80 x 10-2.

Bibliography

1. L.S.Miller, S.Howe and W.E.Spear, Phys. Rev. 166 871 (1968)
2. R.J.Loveland, P.G.LeComber and W.E.Spear, Phys. Lett. 39A 225 (1972)
3. L.Bruschi, G.Mazzi and M.Santini, Phys. Rev. Lett. 28 1504 (1972)
4. L.Emery, C.H.Leung and K.S., J. Phys. C 15 L361 (1982)
5. C.H.Leung, L.Emery and K.S.Song, to appear in Phys. Rev.
6. N.Schwentner et al., Phys. Rev. Lett. 34 528 (1975)
7. B.E.Springett, J.Jortner and M.H.Cohen, J. Chem. Phys. 48 2720 (1968)
8. T.Miyakawa and D.L.Dexter, Phys. Rev. B4 166 (1969)
9. R.F.Wood and H.W.Joy, Phys. Rev. 136 A451 (1964)
10. E.Clementi and C.Roetti, At. Data Nucl. Data Tables 14 (1974)
11. R.H.Bartram, A.M.Stoneham and P.Gash, Phys. Rev. 176 1014 (1968)
12. R.D.Zwicker, Phys. Rev. B 8 2004 (1978)
13. J.C.Slater, Phys. Rev. 81 385 (1951)
14. N.F.Mott and M.J.Littleton, Trans. Faraday Soc. 34 485 (1938)
15. G.A.Cook, Argon, Helium and the Rare Gases, New York: Interscience (1961)
16. S.D.Druger and R.S.Knox, J. Chem. Phys. 50 3143 (1969)
17. Kittel, Intro. to Solid State Phys., J.Wiley and Sons, p. 77
18. R.A.Aziz, Chem. Phys. Letters, 40 57 (1976)
19. Rare Gas Solids vol. II, Academic Press, p.689
20. Rare Gas Solids vol. II, Academic Press, p.800
21. H.R.Glyde, Phys. Rev. B 3 3539 (1971)
22. N.O.Lipari, Phys. Stat. 40 691 (1970)
23. U.Rossler, Phys. Stat. 42 345 (1970)

24. N.O.Lipari and W.B.Fowler, Phys. Rev. B 2 3354 (1970)

25. L.Dagens and F.Perrot, Phys. Rev. B 5 641 (1972)

26. N.O.Lipari, Phys. Rev. B 6 4071 (1972)

27. D.J.Mikish and A.B.Kunz, J. Phys. C 6 1723 (1973))

28. A.B.Kunz and D.J.Mikish, Phys. Rev. B 8 779 (1973)

29. R.N.Euwema, G.G.Wepfer, G.T.Surrat and D.L.White, Phys. Rev. B 9 5249 (1974)

30. N.Erre and R.Resta, J. Phys. C 9 2313 (1976)

31. S.Natalizi and R.Resta, J. Phys. C 10 L477 (1977)

32. M.A.Khan and J.Callaway, Phys. Lett. 73A 441 (1980)

33. S.Baroni, G.Grosso and G.P.Parravicini, Phys. Rev. B 22 6440 (1980)

34. S.Baroni, G.Grosso and G.P.Parravicini, Phys. Rev. B 23 6441 (1981)

35. W.B.Fowler, Phys. Rev. 151 657 (1966)

36. M.Inoue, C.K.Mahutte and S.Wang, Phys. Rev. B 2 539 (1970)

37. A.B.Kunz, Phys. Rev. B 6 606 (1971)

38. Y.Tovozawa, Progr. Theor. Phys.(Kyoto) 12 421 (1954)

39. R.Stewart, J. Chem. Phys. 52 431 (1970)

40. I.shavitt, Methods in Computational Physics vol. 2 p.1-45 (1963)

41. P.Giannozzi, G.Grosso and G.P.Parravicini, Phys. Rev. B 27 7553 (1983)

42. T.Suemoto and H.Kansaki, J. Phys. Soc. Japan 50 3664 (1981)

Abstract

The relative stability of the localized electron state (electron bubble) with respect to the delocalized state (conduction band minimum) in the rare gas solids Ne, Ar and Kr is determined theoretically. The method of the hybrid pseudopotential is used to calculate the energies of the electron bubble and the conduction band state. The method has two basic components. One is the exclusive use of floating ls gaussian basis functions (i.e. the function are not necessarily centered on the atomic sites). The other is the hybrid scheme of representing the effects of the occupied electron orbitals. The deep core electrons are represented by the first two orders of ion-size parameters, first introduced by Bartram et al., while the outer s and p shells are treated exactly as in the extended ion model. A set of efficient and accurate interpolation formulae are proposed to represent the Coulomb, exchange and overlap integrals between the outer shells and the excited electron expressed by a linear combination of floating ls gaussians. The efficiency of the formulae is attributable to the fact that the basis functions are gaussians. The polarization energies for both types of excited states are calculated by the Mott-Littleton method. For the conduction state a slight modification of Fowler's application of the above classical method is made so that the correlation effects from all atoms are taken into account. A quantum mechanical approach used by Kunz was investigated, and was dropped in favor of the much less complex classical method. The electron bubble's electronic structure was determined self-consistently with the atomic displacements.

The solid was considered as a collection of atoms interacting pairwise via standard interatomic potential derived from gas data. For the case of solid Ne only, a simple scheme was developped to approximate the lattice free energy changes once the bubble formed.

Our results for Neon, Argon and Krypton solids agree with experimental evidence that the conduction state is the most stable for these rare gases. Our calculations also suggest that among the rare gases in liquid form, only liquid Ne could support the existence of electron bubbles.